NBSIR 87-3567

Comparisons of NBS/Harvard VI Simulations and Full-Scale, Multi-Room Fire Test Data

John A. Rockett, Masahiro Morita and Leonard Y. Cooper

U.S. DEPARTMENT OF COMMERCE
National Bureau of Standards
National Engineering Laboratory
Center for Fire Research
Gaithersburg, MD 20899

July 1987

U.S. DEPARTMENT OF COMMERCE
NATIONAL BUREAU OF STANDARDS

NBSIR 87-3567

COMPARISONS OF NBS/HARVARD VI SIMULATIONS AND FULL-SCALE, MULTI-ROOM FIRE TEST DATA

John A. Rockett, Masahiro Morita and Leonard Y. Cooper

U.S. DEPARTMENT OF COMMERCE
National Bureau of Standards
National Engineering Laboratory
Center for Fire Research
Gaithersburg, MD 20899

July 1987

U.S. DEPARTMENT OF COMMERCE, Malcolm Baldrige, *Secretary*
NATIONAL BUREAU OF STANDARDS, Ernest Ambler, *Director*

TABLE OF CONTENTS

LIST OF TABLES

LIST OF FIGURES

LIST OF FIGURES (cont.)

LIST OF FIGURES (cont.)

Page

COMPARISONS OF NBS/HARVARD VI SIMULATIONS AND FULL-SCALE, MULTI-ROOM FIRE TEST DATA

John A. Rockett, Masahiro Morita and Leonard Y. Cooper

ABSTRACT

The NBS/Harvard VI multi-room fire model computer code was used to simulate results of previously reported full-scale, multi-room fire experiments. The tests and simulations involved: four different compartment configurations made up of two or three rooms connected by open doorways, four different fire types generated by a methane burner located in the room identified as the burn room, and up to four different doorway openings between the burn room and the adjacent space. A total of nineteen different tests were carried out and simulated. Comparisons between simulated and measured parameters of the fire-generated environments are reviewed. While the computer code is generally found to provide favorable simulations for the entire range of tests, several areas in modeling detail are identified as requiring clarification, research, and further improvement. The improvements should be incorporated in future versions of the NBS/Harvard Multi-Room Fire Model.

Key words: Computer models; compartment fires; fire models, full-scale fire; multi room fires; simulation; validation

1. INTRODUCTION AND OBJECTIVE

The NBS/Harvard VI compartment-fire simulator is a computer code which predicts the dynamic environment generated by fires in multi-room enclosures. The development of the computer code in its original Harvard VI form [1,2] was carried out at Harvard University as an outgrowth of the Harvard V, single-room compartment fire simulator [3,4]. The continued development and further enrichment of the code is being carried out at the Center for Fire Research of the U.S. National Bureau of Standards [5].

Reference [6] describes the results of an extensive series of full-scale, multi-room enclosure fire tests. The purpose of the work reported here was to use the NBS/Harvard Code to simulate the results of this experimental study and to describe and analyze the results of a comparison between the predictions and the actual data tabulated in [6].

2. DESCRIPTION OF THE TESTS

The following description of the test program is a summary of the presentation in [6]. The reader is referred to that work for additional clarification.

The test program of [6] consisted of a series of separate tests involving a variety of compartment configurations and fire energy release rates. For a given test, the compartment involved either two or three rooms, all having a nominal 2.36 m ceiling height, connected by open doorways. The wall and ceiling surfaces of all rooms were lined with 0.013 m thick gypsum board, and the floors were concrete. During the course of the test program the space was partitioned to yield four different configurations ranging in total plan area from 40.6 m^2 to 89.6 m^2. These configurations are sketched in Fig. 1. The doorway between the burn room and its adjacent space (designated as the corridor) was 2.0 m high and 1.07 m wide. The doorway between the corridor and the next adjacent space (the lobby) was 2.01 m high and 1.32 m wide.

An attempt was made to seal cracks and penetrations in the bounding surfaces of the test space. A 0.15-m (high) x 0.94-m (wide) hole with clear opening to the outside (through an unused room and open window of the test facility) was provided next to the floor in a wall surface of the corridor. The hole was to provide the major leakage path for mass exchange between the test space and the outside environment.

Each test used the same burn room of 14.0 m^2 area. The room contained a 0.30 m x 0.30 m square methane diffusion burner whose surface was positioned 0.24 m above the floor and approximately in the center of the room. After ignition from a pilot flame, fuel supply to the burner was controlled manually from an outside metering system to produce one of four energy release rates: a constant rate, Q, of 25 kW, 100 kW, or 225 kW; or a time varying energy release rate, $Q_{ramp}(t)$, of

$$Q_{ramp}(t) = 30\ t\ kW,\ 0 \leq t\ (t\ in\ minutes) \qquad (1)$$

where the time from ignition, t, never exceeded 10 min.

The free-burn characteristics of the particular burner used in these tests were studied in [7]. Using methane for a fuel, and for fires between 50 kW and several hundreds of kW, it was found that, of the total energy release rate of the fire, a fraction, λ_r, of approximately 0.24 is radiated away from the combustion zone. For a 25 kW fire λ_r was found to be 19 percent.

With methane as a fuel the burner produced very little smoke. In order to have a visual tracer of the combustion products as they spread throughout the compartment, an artificial source of smoke (a commercially available, non-toxic smoke candle) was introduced into the ceiling jet of the burn room. Thus, in every test, a highly visible white smoke was generated by a smoke candle and mixed with the fire's products of combustion near their source for up to 5 min. Effective visualization of the upper smoke layers was achieved by placing fluorescent light fixtures on the floor of the corridor and lobby.

For each of the four spatial configurations of Fig. 1, a separate burn test was run for each of the four energy release rates (16 test runs). For the 100 kW fire and full corridor configuration of Fig. 1, three additional tests were also run. In these tests, the burn room-to-corridor doorway width was reduced to 1/2, 1/4, and 1/8 of its full value of 1.07-m.

The test instrumentation is described in detail in [6]. It consisted of five thermocouple "trees" located as shown by A-E in Fig. 1. There were eight thermocouples on each tree and, except for the doorway, they were 0.30 m apart, the lowest one being 0.15 m from the floor and the uppermost 0.07 m from the ceiling. Photometers measured the growth of the smoke layer, and video tapes were made during each test allowing post-test analysis of the smoke layer growth by noting the extent of smoke obscuration of vertical scales mounted within the field of vision of the cameras (at positions V of Fig. 1). A single pair of pressure taps located at A and C (see Fig. 1) measured the pressure difference between the burn room and the corridor at the ceiling elevation.

3. TEST RESULTS AND THE PARAMETERS SIMULATED

The NBS/Harvard VI code simulates the fire-generated environment within each room of a compartment as having two homogeneous horizontal gas layers separated by a sharp interface: an elevated temperature, combustion-product-contaminated (i.e., smoky) upper layer and a lower layer of uncontaminated air at ambient temperature. Observations during the reference [6] tests and during other, similar fire tests suggest that this two-layer description is frequently a reasonable, albeit distinctly idealized approximation of the actual phenomena. The approximation is idealized in that the actual interface between the gas layers is not sharp. In some cases there is a relatively narrow, in others a relatively broad transition region across which the gas temperature, smoke opacity and product of combustion densities change. Further, in many fires, the gas in the lower part of the rooms is, at later times, neither free of smoke nor at ambient temperature [6,8,10].

Reference [6] uses three rules for defining a layer interface height based on the experimental data: (1) the height at which the gas temperature rise above ambient is N percent of the temperature rise at the topmost thermocouple or at least 0.5 K; (2) an analogous rule applied to the photometer data; and (3) visual observation as determined from video tapes. In [6], data for selected runs and at selected thermocouple locations are used to provide the time-dependent interface heights based on rule 3, and based on rules 1 and 2 for N = 10, 15, and 20. Tabulated interface heights according to rules 1 and 2 for N = 10, and to rule 3 are provided in [6] for each room during all nineteen tests.

Reference [6] presents vertical temperature distributions for only one of the nineteen tests, and for this at only one corridor thermocouple tree location and at only one instant of time. In general, only three time-varying measures of the thermocouple tree data are presented for each room during all runs. The first of these measures is the floor-to-ceiling-averaged temperature. As it turned out, for each test, the history of this vertically averaged tempera-ture was found to be substantially the same at all (up to three) thermocouple tree locations in the corridor. Accordingly, only the vertically averaged temperatures at location D are tabulated for the corridor in [6] and reported in this work. The second measure of the dynamic temperature distribution in the test spaces is the above-mentioned interface

elevation according to rule 1 with N = 10. The third dynamic measure of the thermocouple data is a result of analysis on the first of these measures. This leads to estimates of the instantaneous total rates of heat transfer to bounding surfaces of the test space (given in terms of a fraction, λ, of the instantaneous burner power output) which are tabulated in [6] for all test runs.

Five types of comparisons between NBS/Harvard VI simulations and the experimental data are presented in this paper. In one, the histories of predicted floor-to-ceiling-averaged temperatures are compared with the corresponding histories as tabulated in [6]. The second type of comparison involves predicted two-layer interface elevations and experimentally determined, N = 10 interface elevations. Thirdly, the vertical distribution temperature test data (archived at the National Bureau of Standards) were consulted. For a few test scenarios and at the arbitrarily selected test time of 200 s, these are compared to the predicted temperature distributions. The fourth type of comparison is between the experimental and predicted time-varying rate of total heat transfer loss to the bounding surfaces of the test space. Finally, comparisons are made between experimental and predicted near-ceiling, cross-wall, burn-room-to-corridor pressure differentials.

Each of the nineteen tests are indicated by groups of numerical entries in Table 1. Simulations were carried out for all runs. The entries in the table refer to the numbers of the figures (to be introduced and discussed below) in which the above-mentioned comparisons between simulation and test data are displayed.

The input data for the computer runs are presented in Table 2.

4. PRESENTATION OF THE TEST DATA AND THE PREDICTIONS

The first simulation results to be presented will be for the 100 kW fire, full corridor and lobby test configuration with full burn room-to-corridor doorway. For each of the three rooms, computed results and corresponding experimental data for the time-dependent interface elevations are plotted in Figure 2a. Plotted in Figure 2b are (1) the computed and measured vertically-averaged temperature rise histories based on thermocouple tree data at locations A, D and E as noted on figure 1: ΔT_A(burn room), ΔT_D (corridor), ΔT_E (lobby), (2) the burn room-to-corridor cross-doorway pressure differential, Δp, and (3) the heat transfer parameter, λ. The heat transfer parameter λ is defined as the fraction of Q(t) which is lost by radiation and convection to the bounding surfaces of the test space. $\lambda(t)$ is estimated from the $\Delta T(t)$ data and Q(t) according to Eqs. (4) and (5) of [6].

Figure 3 compares the predicted and measured vertical temperature distributions in the three rooms at 200 seconds. As mentioned earlier, the 200 second experimental data, which are not documented in [6], were obtained from magnetic tapes archived at NBS.

Plots similar to Figure 2a and 2b are provided in Figures 4-21 for the remaining 18 tests of Table 1. Discussion of these results will be presented in the next section along with results of selected additional simulations involving variants in the original calculations.

5. DISCUSSION OF RESULTS AND ADDITIONAL SIMULATIONS

5.1 Orifice Coefficients and the Subdivision of Large Spaces

Typical applications of zone compartment fire models tacitly assume that openings (vents) between contiguous spaces are small enough that flows through them can be modeled as orifice-type flows (constant orifice coefficient) between relatively quiescent regions. If a vent is too large (e.g., if the width of the vent approaches the characteristic width of either of the contiguous spaces) then some modification to the analysis is appropriate. Analysis and experimental results presented in [9] suggest that an adequate modification in this regard involves a variable rather than a constant orifice coefficient; the coefficient varies, approaching unity as the ratio of vent opening width to exiting room width approaches unity.

Consistent with the above, the NBS/Harvard VI code incorporated the orifice coefficient formula recommended in [9]. To test this new capability the 100 kW, burn room-corridor-lobby test was simulated a second time. This test was chosen for comparison because, in this case, the predicted burn room average temperature rise was in good agreement with the experiment whereas the burn room-to-corridor pressure difference was not. The corridor test space was conceptually partitioned into three identical, contiguous spaces with joining vents having the full corridor width and height 10 cm less than the corridor height. (10 cm was used based on previous, unpublished experience in simulating corridor flows.) The center corridor section (Room 3, per the 3-space corridor data of Table 2) included the doorway vent to the burn room and the pressure tap. It also shared a "full" vent with each of the two end sections, one a "deadend" (Room 2, the left portion of the corridor as seen in Figure 1) and one with the doorway to the lobby (Room 4, the right portion of the corridor as seen in Figure 1).

Results of the new fire-room simulation are plotted in Figure 22a (layer heights) and Figure 22b (vertically averaged temperatures, cross-door pressure differential and heat transfer parameter). These two Figures are to be compared to Figures 2a and 2b, respectively. Review of these results leads to the following observations:

There is a slight difference between calculated values of lobby and burn room layer heights, plotted in Figures 2a and 22a, and of Δp, λ and ΔT_A plotted in Figures 2b and 22b.

Due to the amount of scatter in the data, it is not possible to tell if subdividing the corridor improves the layer height simulation. The predicted average

temperature rises vary along the corridor more than the measured values ΔT_C and ΔT_D at the locations C and D indicated in Figure. 1.

The predicted ceiling pressure difference between the burn room and the corridor sub-room in which the corridor pressure was measured is in better agreement with the data than that for the undivided corridor.

The computed burn room-to-corridor pressure difference exceeds the measured values as shown in Figure 2 and Figures 4-21 for all the tests except those for the smallest (25 kW) fire, Figures 7-10. The discrepancy increases with fire size. While this could have resulted from inadequately sealed leaks in the burn room, the improved agreement for the subdivided corridor simulation suggests that this was probably not the case. Rather, the slight pressure change along the corridor as one moves away from the burn room door is more likely responsible. (Note that the gas flow in the corridor upper layer is away from the burn room door in both directions; the corridor ceiling pressure is highest near the door and, therefore, the burn room-to-corridor pressure difference is smallest there. Thus, the average burn room-to-corridor pressure difference should be smaller than the local burn room-to-corridor pressure difference just outside the door.) This is partially compensated for by subdividing the corridor. Bearing this in mind, the predicted and measured pressure differences are satisfactory.

5.2 Temperature Rise and Overall Heat Losses

Figures 2b and 4b-21b show the vertically averaged temperature rise in the several rooms. The most striking feature observed on comparing these Figures is the distinct break in the computed temperature rise for the larger fires in the smaller spaces which is not reproduced in the data. (See, for example, Figures 8b,9b and 10b as compared to Figure 2b, Figures 14b through 17b and Figures 18b through 21b). This is due to an inadequate treatment in the modeling of "oxygen limited burning". The simulation always models the upper layer gas as being so depleted of oxygen that it will not support combustion. For the cases considered here and, indeed, for many other scenarios, the assumption is not adequate. Thus, in a simulation, when the upper layer descends to the height of the surface of a burning object (in the present case, the burner), the object continues to pyrolyze, but none of the fuel evolved is assumed to burn. This is in difference to the fact that until much of the upper layer oxygen is used up, burning rate will not be reduced significantly. This defect in the simulation has been identified for correction in a revised version of the simulation. All predicted results presented here should be disregarded beyond times of the above-mentioned "breaks."

In a number of the cases, the predicted temperature rises faster at the beginning of the test than the experimental data (Figures 2, 7, 8 and 19). This is by no means always the case, however, as shown by Figures 5, 20 and 21. In Figure 8 the experimental temperature data suggests that the gas flow

to the burner was decreased slightly at about 150 seconds. Taken together, these results suggest that manual adjustment of the gas flow to the burner did not produce as rapid a build-up to steady gas flow rate as assumed in the calculation.

The gas burner algorithm does not account properly for the heat needed to bring the burner itself to operating temperature. If the algorithm were improved in this respect the temperature would rise somewhat more slowly than it now does. This would improve agreement with some tests and make it less satisfactory for others.

Besides the above, two distinct trends appear when comparing the simulation results with the experimental data. One is observed as fire size varied, the other, as the burn room door size varied. As for the first (Figures 2, 7 and 17 and Figures 3 and 25), the simulation seems to predict higher-than-measured burn room temperatures for the larger fires, and smaller ones for the smaller fires. The reverse tendency may be present in the corridor and lobby although the temperature rise is so small in these spaces that this is somewhat less obvious. For the ramp fires (Figure 21), the prediction lies consistently above the experimental data for all times.

The λ plots indicate no consistent trend in comparisons of measured and predicted heat loss to the boundary surfaces of the compartment. For these, there is general agreement between the experiments and simulations after an initial period. The λ calculation is for heat losses throughout the entire space. Thus, for any given test run, good agreement between measured and predicted values of λ could be obtained, for example, even if predicted losses were over-estimated significantly in the burn room and under-estimated significantly in the other spaces. Were it not for the ramp fires, where the trend is uneven, the λ plots together with the average temperature rise plots suggest that the simulation heat transfer is under-estimated for the higher temperatures, and over-estimated for the lower ones. In assessing simulation λ values versus those values derived from experiment, note that in the experimentally derived values, temperatures at only one location in each of the rooms were used. This may limit significantly the accuracy of the measured values of λ. On the other hand, many approximations are embedded in the λ estimate of the simulation and these may limit significantly its accuracy.

Tests 10-13 varied the burn room door size. Figures 10-13 and Figures 3 and 23 compare the experimental and simulation results for these tests. The simulation underestimated significantly the burn room temperature for the smallest door, with improving agreement as the door is increased in size. There are three possible reasons for this discrepancy. First, the simulation does not include the effect of mixing between the hot gas exiting from the room and cool gas entering. (Mixing of the exiting upper layer gas with that entering the lower layer through the same vent.) It has been shown that this can be important [8] and, when modeled [10], raises the gas temperature in the burn room. The effect would be more pronounced for the smaller doors. The second possible reason involves the door flow algorithm. The data suggests that too much flow exits from the narrower doors. Note, however, that data for steady gas burner fires in a room with various openings [11] was well-

modeled by the same door flow algorithm used here [10]. The third reason relates to the overall modeling of convective heat transfer. In the present model a single heat transfer coefficient is used where this is based on the difference between the (average) upper layer temperature and that of the (average) ceiling surface. The actual convective heat transfer is driven by the differences between plume-driven ceiling/wall boundary flow temperatures and ceiling wall surface temperatures. These latter temperature differences and the corresponding distribution of heat transfer coefficient can be expected to vary significantly from peak values at plume-ceiling impingement to relatively low values at distant ceiling and upper-wall surface elements [12-15]. A more detailed model for the upper layer-to-ceiling convective heat transfer might improve agreement for these and other tests. It is also likely, that such a model would have an impact on the aforementioned simulation λ estimates.

Figures 3, 23, 24 and 25 present typical vertical temperature profiles together with the corresponding simulation result. For the burn room, the experimental data clearly show two nearly-isothermal gas layers separated by a roughly 20 cm thick transition region. The predicted layer depth is in satisfactory agreement with the data. Note that in each case there is some increase in lower layer temperature above ambient. For the case of the 100 kW fire (Figure 3), where the measured and predicted average temperature rise are in best agreement, this agreement is obtained from a predicted upper layer temperature which is too high combined with a lower layer temperature which is too low. Were layer mixing at the vent included, the lower layer temperature would rise due to the effects of mixing. Also, the predicted upper layer temperature would be expected to rise somewhat due to decreased radiation heat loss through the lower layer to the floor. For constant fire size, narrowing the vent increases the mixing; Figures 3 and 23 illustrate this. For constant vent size, decreasing the fire size decreases mixing; Figures 3 and 25 illustrate this.

No attempt was made to simulate the effect of the smoke candle. (Note that no test was re-run without artificial smoke to assess its effect.) Raising the smoke production significantly above that for a relatively weakly radiating methane fire would have lowered the predicted upper layer temperature, the effect being more pronounced for the larger fires.

While the two-layer model seems satisfactory for the burn room, the vertical temperature data for the corridor and lobby (Figure 3) show that, away from the burn room, the assumption of two distinct, isothermal gas layers is a much more questionable idealization. The two-layer model is based on the assumption of well-mixed layers. In reality, the process by which the hot layer is formed seems to involve the development of successive, stably stratified layers [17, 18]. When hot gas first enters a compartment it spreads as a "gravity current" under the ceiling to form a thin, nearly uniform thickness hot layer. This spreads until it reaches the compartment walls where it turns flowing back under itself. During this process the gas forming the ceiling layer loses heat to the ceiling and may be mixed with the cool gas already present in the room. We may think of one "complete ceiling layer" to have been formed when the returning flow reaches the entry point. A second layer then begins to form over the earlier one. The newest, hottest

layer forms under the ceiling pushing the older layers down as it forms. Where there are suitable vents, the bottom-most layers may be siphoned off and cool gas allowed to enter the lower part of the room. Eventually, as the temperature difference between the newest and older layers decreases, a nearly isothermal layer "stack" may be found. However, for times allowing only the initial filling process to occur, this fill mechanism will not produce a pair of well-mixed layers. Thus, it is not to be expected that the two-isothermal-layer model, based as it is on the assumption of well mixed layers, would be entirely satisfactory for the corridor and lobby for tests studied here. For the corridor and lobby a more detailed transient model for the layer growth may be desirable. Even so, as will be shown in the next section, the two layer model does seem to give adequate overall predictions of the temperature and layer depth in these spaces.

5.3 Layer Depth Comparisons

Turning now to the layer depth comparisons (figures 2a - 22a), the computed layer interface heights are seen to be generally higher than those given by applying the 10 percent temperature rise rule to the experimental data. Where the temperature data suggests a more rapid fire buildup for the calculation than the actual fire, the computed layer descends more rapidly than the data indicates. This is to be expected if the computed and actual fires do not develop in the same way, as already discussed. Otherwise the comparisons are satisfactory. The computed layer depths depend on the plume entrainment algorithm used. In NBS/Harvard VI the plume arises from an area source, calculated using a virtual point source located below the actual fire surface height. Alternate plume models might be used and different layer depths predicted [16]. It is possible that some improvement might be found. However, to date, no provision has been made in NBS/Harvard VI to change the plume model.

If the layer depths are too small, the layer temperature will be high. However, the vertically averaged temperature will be much less sensitive to changes in layer depth. Changing the plume model, while possibly improving the layer depth agreement, would alter the other results. A plume model which increased layer depth would increase the door flows. This would increase the convective heat loss from the burn room, lower its average temperature and raise the temperature in the adjacent spaces. Considering the scatter of the experimental data, the results are satisfactory. They do, however, suggest use of either a layer interface definition by the "N percent rule" [6] with N greater than the 10 percent or an alternate plume algorithm.

The use of artificial smoke to allow the hot layer behavior to be visually tracked was not simulated in the calculations use and may have influenced the comparisons. This would be expected to have more influence on the configurations producing higher upper layer temperatures than those where upper layer temperatures were lower. The simulation can treat gas as well as particulate radiation and, with empirically-altered input data to account for the artificial smoke, it might have produced for favorable comparisons. However, the empirical adjustment of input to produce a "best fit" to

experimental data must be used with caution when assessing the capability of a model. This was not done here.

6. CONCLUSIONS

The simulations generally compare favorably with the experiments. As the compartment geometry or fire size were varied the trends found experimentally were reproduced by the simulations. There were differences in detail, however. In some cases the experimental data and simulations differed in ways that are most likely due to differences between assumed and actual experimental conditions. For example, in the burner gas flow rate during the first two minutes of the fire, and the radiation from the natural gas fire and its plume which was assumed to be negligible, but which, due to the use of artificial smoke, may not have been.

A known weakness of the simulation is its modeling of "oxygen limited burning" which came into play here for the larger fires in the smaller spaces. This is a known weakness of the simulation, scheduled for rectification. Revised physics to account more properly for burning at times when the hot gas layer nearly reaches or even envelopes a burning object should be included as soon as possible.

Mixing of the hot and cool layer gases as they pass through a vent should be included in the simulation. Mixing occurs on both sides of a vent and both should be included. This would likely improve the agreement between the experimental data and the predictions studied here, especially in the partially open burn room door cases.

More detailed modeling of convective heat transfer could lead to significant improvements in all aspects of temperature predictions. This is especially true for fire scenarios, like the ones studied here, where temperature increases of the upper layers are not so high that radiation dominates the heat transfer processes (e.g., fire scenarios where upper layers are within a few hundred K above ambient).

Provision for the use of alternative plume entrainment algorithms should be considered. It is possible that use of a different available algorithm might lead to better agreement with experiment.

The variable orifice coefficient capability of NBS/Harvard VI will be useful in simulating fire-generated environments in corridor spaces having segments with different cross-sections, or in other large area spaces having irregular floor plans or varying ceiling heights.

Improvement of the gas burner algorithm to account for the heat absorbed by the burner body early in the fire is worth considering.

Perhaps the most important conclusion of this study is that the NBS/Harvard VI multiroom compartment fire model computer code can be expected to provide useful predictions of fire-generated environments in multiroom fire

scenarios similar to those studied experimentally in [6]. These can be characterized mainly by fire sizes on the order of several hundred kW and total room areas of the order of 100 m^2.

7. REFERENCES

[1] Gahm, J.B., "Computer Fire Code VI", NBS-GCR-83-451 (2 volumes), U.S. Department of Commerce, Nat. Bur. of Stands., Gaithersburg, MD 20899, December 1983.

[2] Ramsdell, J., "Variable Elimination in the Home Fire Code", ASME/AIChE National Heat Transfer Conferences, paper 81-HT-3, Milwaukee, Wisconsin, Aug. 2-5, 1981.

[3] Mitler, H., "The Physical Basis for the Harvard Computer Fire Code", Home Fire Project Technical Report No. 34, Division of Applied Sciences, Harvard University, Cambridge, MA, October 1978.

[4] Mitler, H.E. and Emmons, H.W., "Documentation for CFC V, The Fifth Harvard Computer Fire Code", Home Fire Project Technical Report No. 45, Division of Applied Sciences, Harvard University, October 1981.

[5] Rockett, J.A. and Morita, M., "The NBS/Harvard VI Multi-Room Fire Simulation", Fire Science and Technology, Vol 5, No 2, 1985 (159-164), Tokyo, Japan.

[6] Cooper, L.Y., Harkleroad, M., Quintiere, J.G. and Rinkinen, W., "An experimental study of upper hot layer stratification in full-scale multiroom fire scenarios", Jour. of Heat Transfer, Vol. 104, p. 741, November 1982.

[7] McCaffrey, B., "Measurements of the Radiative Power Output of Some Buoyant Diffusion Flames", Western States Section, Combustion Institute, WSS/CI 81-15, Pullman, WA, 1981.

[8] McCaffrey, B.J. and Rockett, J.A., "Static pressure measurements of enclosure fires", Jour. of Research of the Nat. Bur. of Stands., Vol. 82, No. 2, p. 107, 117, Sept.-Oct. 1977.

[9] Steckler, K.D., Baum, H.R. and Quintiere, J.Q., "Fire Induced Flow Through Room Openings - Flow Coefficient", NBSIR 83-2801, U.S. Nat. Bur. of Stands., Gaithersburg, MD 20899, March 1984.

[10] Rockett, J. A., "Modeling of NBS Mattress Tests With the Harvard Mark V Fire Simulation", Fire and Materials, Vol 6, No 2, pp 80-95, June 1982

[11] Steckler, K.D., Quintiere, J.G. and Rinkinen, W.J., "Flow Induced by Fire in a Compartment", NBSIR 82-2520, U.S. National Bureau of Standards, Washington, D.C., Sept. 1982

[12] Alpert, R.L., Fire Induced Turbulent Ceiling-Jet", FMRC Serial No. 19722-2 May 1971, Factory Mutual Research Corporation, 1151 Boston-Providence Turnpike, Norwood, MA 02062

[13] Veldman, C.C., Kubota, T. and Zukoski, E.E., "An Experimental Investigation of the Heat Transfer from a Buoyant Gas Plume to a Horizontal Ceiling - Part 1, Unobstructed Ceiling", NBS-GCR-77-97 Part 2, Effects of Ceiling Layer, NBS-GCR-77-98 U.S. Nat. Bur. of Sts., Washington, D.C., 1977

[14] Cooper, L.Y., "Heat Transfer from a Buoyant Plume to an Unconfined Ceiling", Journal of Heat Transfer, Vol 104, Aug., 1982

[15] Cooper, L.Y. and Stroup, D., "Thermal Response of Unconfined Ceilings Above Growing Fires and the Importance of Convective Heat Transfer", Journal of Heat Transfer, Vol.109, Feb., 1987.

[16] Rockett, J.A., McCaffrey, B.J. and Levine, R., "Naval fire fighting trainers: Effect of ventilation on fire environment (Model calculations for 19F3 FFT)", NBSIR 85-3238, U.S. Nat. Bur. of Stds. Washington, D.C., December 1985

[17] Tangren, E.N., Sargent, W.J. and Zukoski, E.E., "Hydraulic and Numeric Modeling of Room Fires", Daniel and Florence Guggerheim Jet Propolsion Center, California Institute of Technology, Pasadena, CA, June, 1978.

[18] Zukoski, E.E., and Kubota, T., "Experimental Study of Environment and Heat Transfer in a Room Fire, Final Report", California Institute of Technology, Division of Engineering and Applied Science, Pasadena, CA July 1984.

Table 1. Figure Numbers Versus Test Parameters

Fire	Configuration						
	1/2 Corridor	3/4 Corridor	Full Corridor	Full Corridor 1/2 Door	Full Corridor 1/4 Door	Full Corridor 1/8 Door	Full Corridor and Lobby
25 kW	4	5	6				7, 25
100 kW	8	9	10	11, 24	12, 24	13, 23	2, 3, 22
225 kW	14	15	16				17, 25
Ramp	18	19	20				21

Table 2. Input Data

Fuel Properties:

Heat of combustion	55.5	MJ/Kg
Fraction of heat released	0.99	
Stoichiometric air/fuel mass ratio	17.25	
Gr CO2 produced per gr fuel burned	2.75	
Gr H2O produced per gr fuel burned	2.25	
Gr CO produced per gr fuel burned	0.019	
Gr soot produced per gr fuel burned	0.008	
Flame absorption coefficient	1.55	1/m

Thermal Properties of Walls:

Thickness	0.0254	m
Density	800.	kg/m_3
Specific heat	1062.	J/kg-deg C
Thermal conductivity	0.134	W/m-deg C

Room Dimensions:

Single Space Corridor

Rm. 1 - burn room:	4.22 x 3.35 x 2.44 high
2 - full corridor:	18.97 x 2.41 x 2.44
2 - 3/4 corridor:	14.23 x 2.41 x 2.44
2 - 1/2 corridor:	9.48 x 2.41 x 2.44
3 - lobby:	3.00 x 15.40 x 2.44

3-Space Corridor

1 - burn room:	4.22 x 3.35 x 2.44
2 - left corridor:	6.32 x 2.41 x 2.44
3 - middle corridor:	6.33 x 2.41 x 2.44
4 - right corridor:	6.32 x 2.41 x 2.44
5 - lobby:	3.00 x 15.40 x 2.44

Vent Geometries:

Single Space Corridor*

Rm 1 - Rm 2:	1.07 x 2.03 high	(full door)
1 - 2:	0.54 x 2.03	(1/2 door)
1 - 2:	0.27 x 2.03	(1/4 door)
1 - 2:	0.13 x 2.03	(1/8 door)
2 - 3:	1.25 x 2.01	
2 - outside:	0.94 x 0.15	

*Rm 1 - burn room
Rm 2 - corridor
Rm 3 - lobby

3-Space Corridor**

Rm 1 - Rm 3:	1.07 x 2.03 high
2 - 3:	2.41 x 2.43
3 - 4:	2.41 x 2.43
4 - 5:	1.25 x 2.01
3 - outside:	0.94 x 0.1

**Rm 1 - burn room
Rm 2 - left corridor
Rm 3 - middle corridor
Rm 4 - right corridor
Rm 5 - lobby

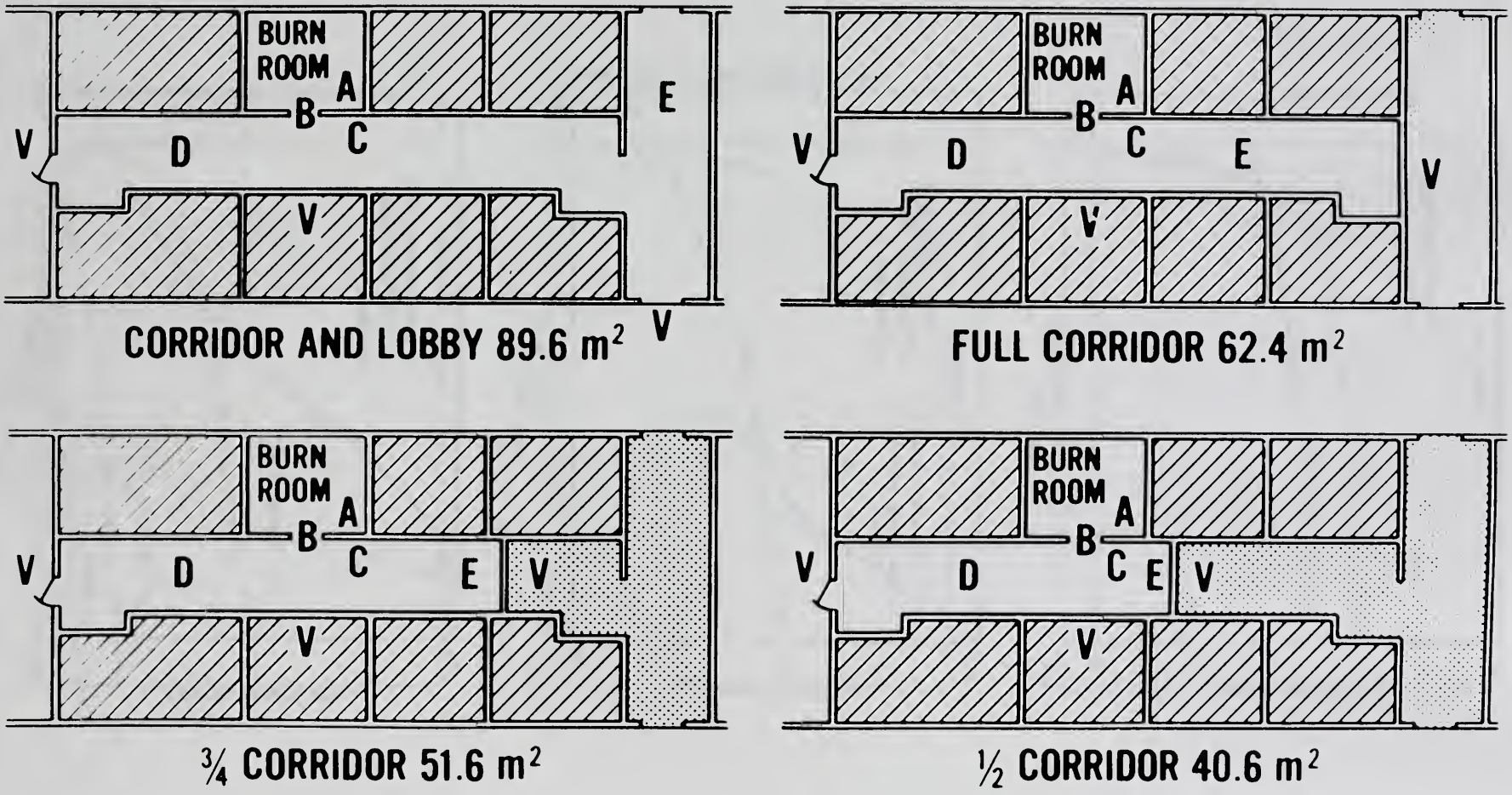

Figure 1. Sketches of the four test configurations with indications of the locations of vertical instrument arrays (A,B,C,D, and E) and of video cameras (V)

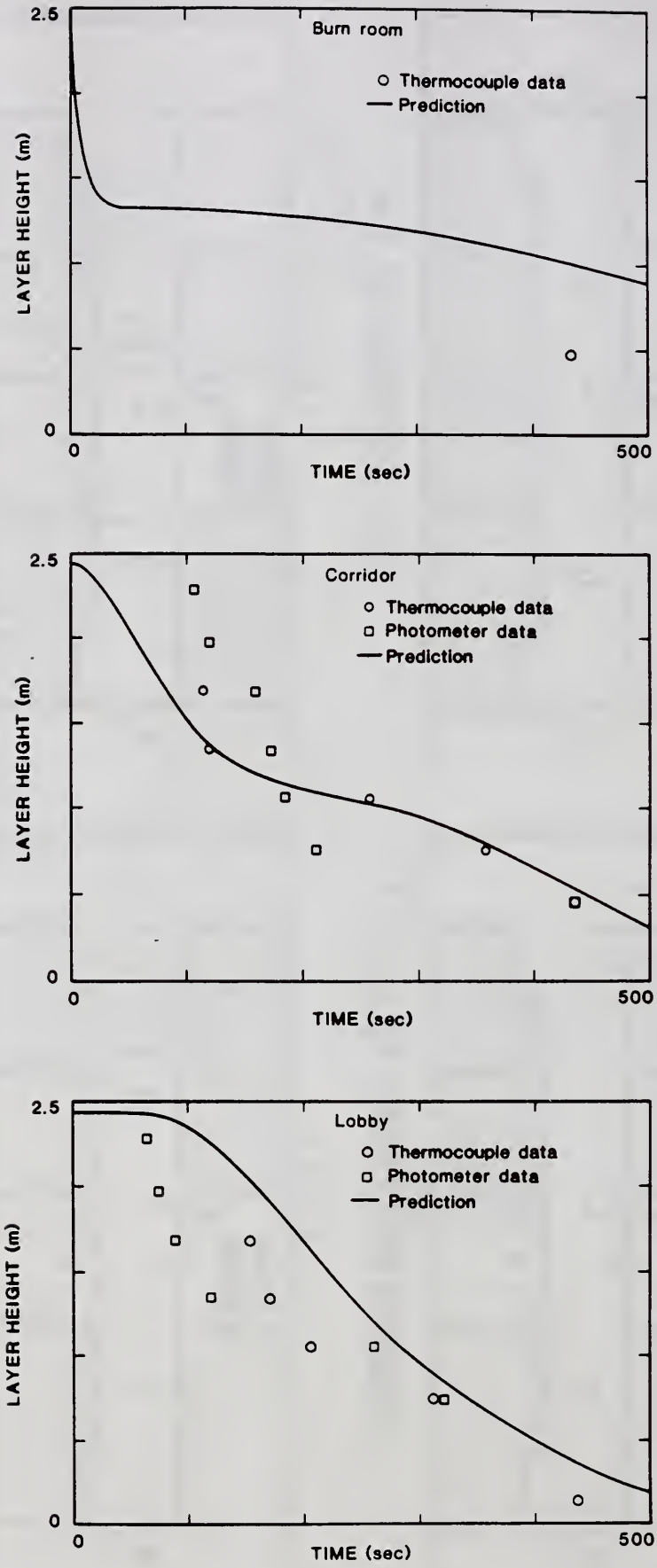

Figure 2a. 100 kW fire, Corridor and Lobby configuration: layer heights.

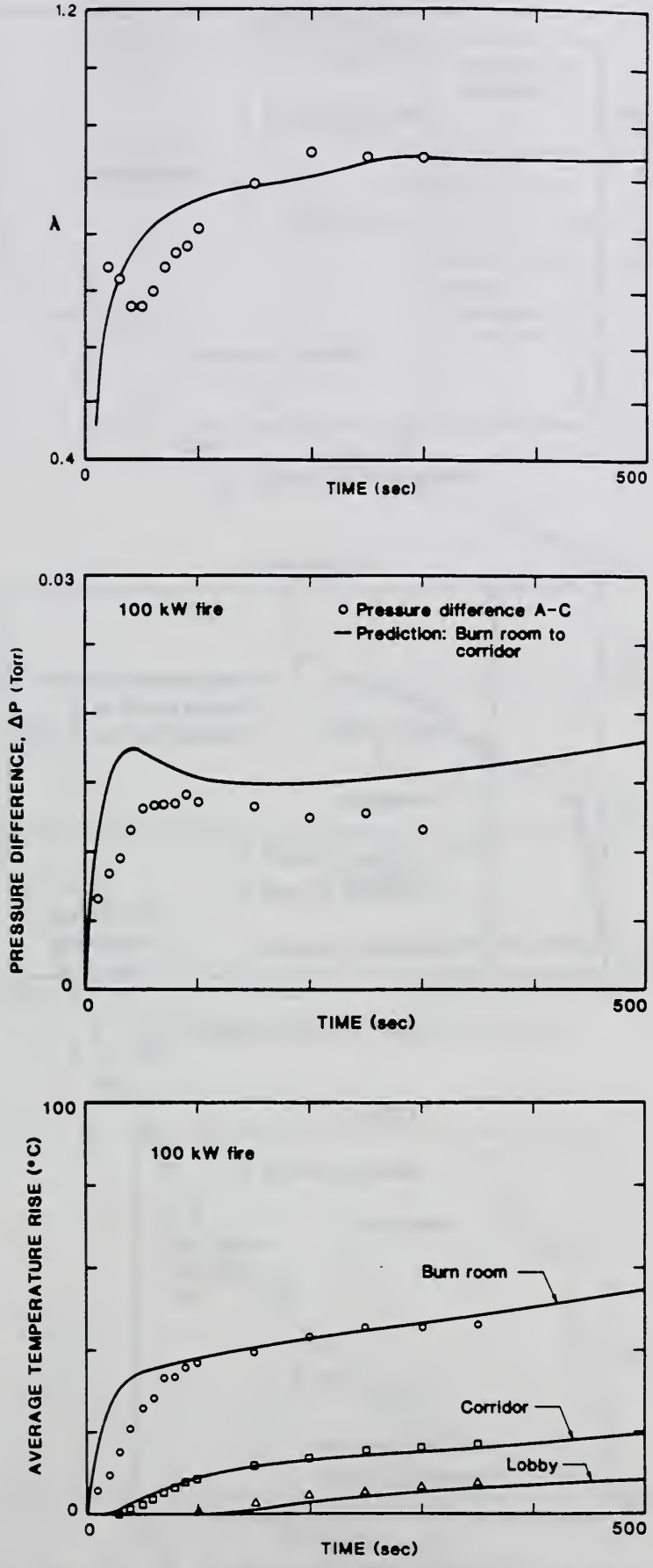

Figure 2b. 100 kW fire, Corridor and Lobby configuration: λ, pressure difference and average temperature rises.

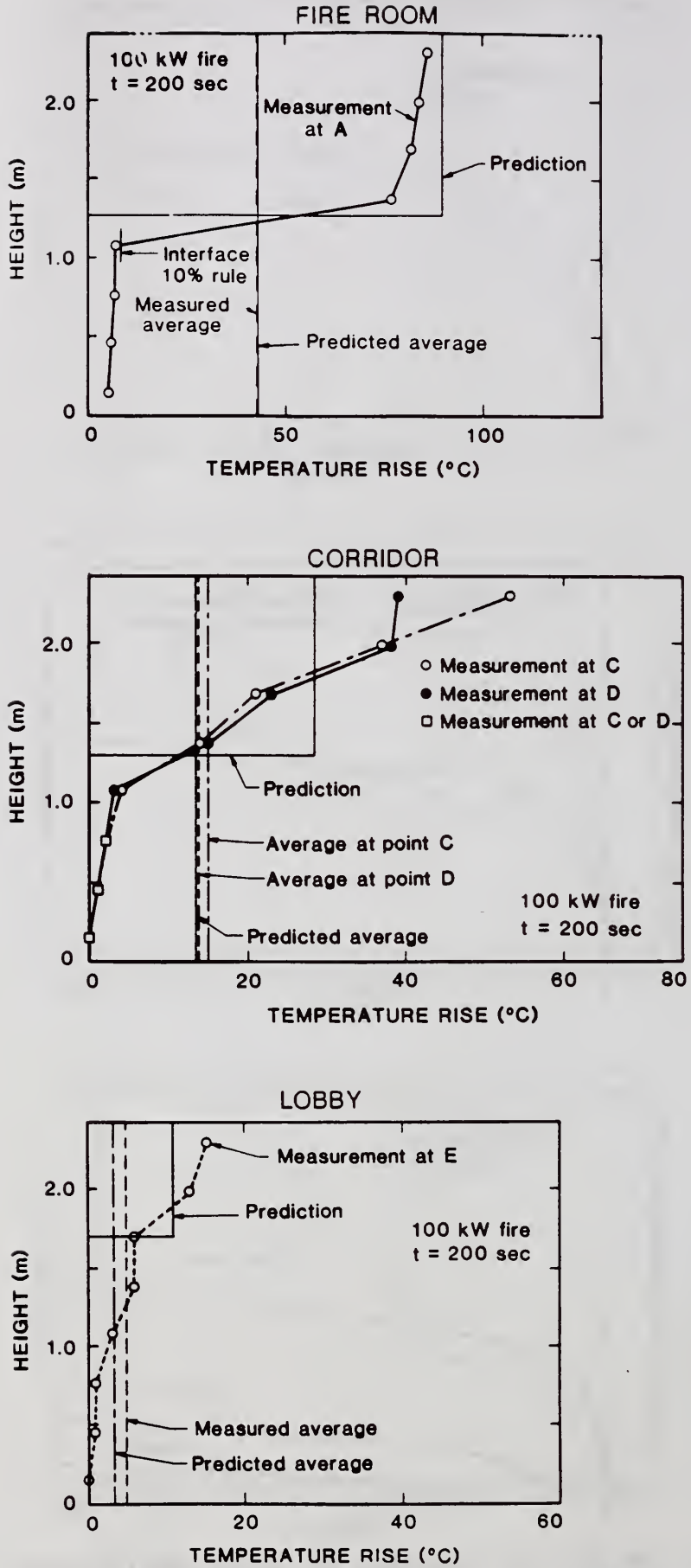

Figure 3. Vertical temperature profiles, 100 kW fire, Corridor and Lobby configuration at 200 sec.

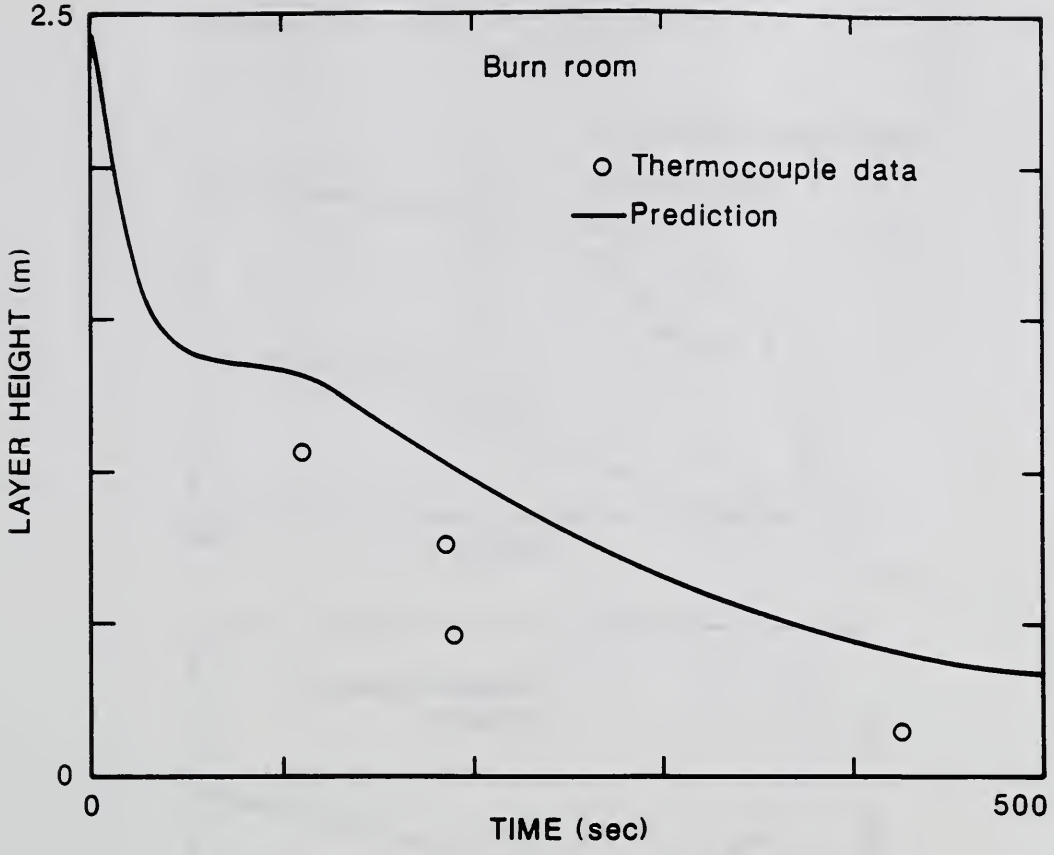

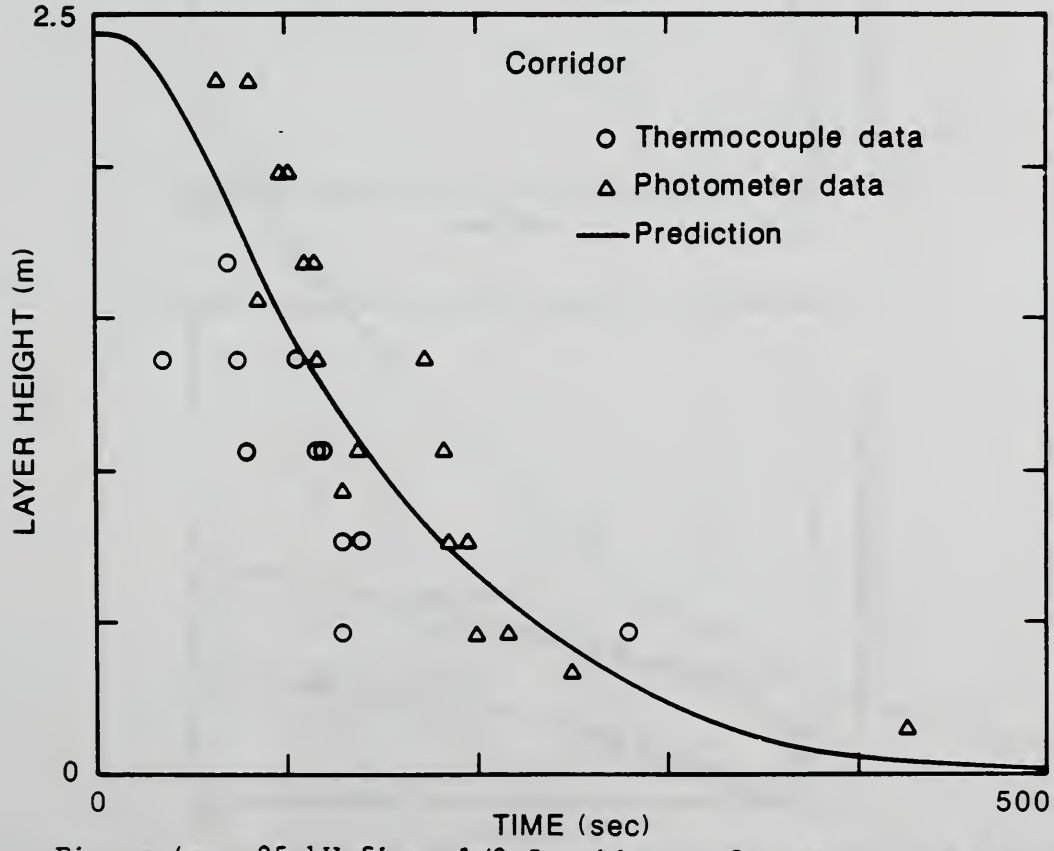

Figure 4a. 25 kW fire, 1/2 Corridor configuration: layer heights.

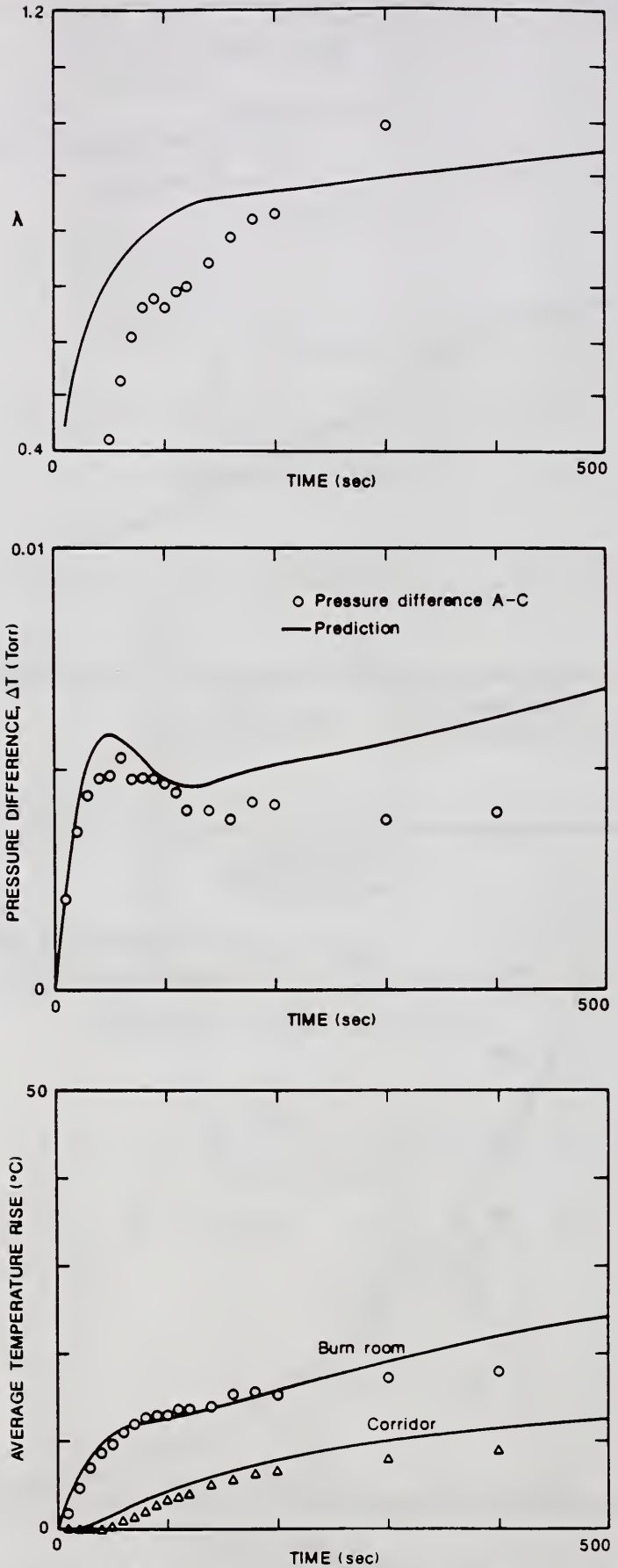

Figure 4b. 25 kW fire, 1/2 Corridor configuration: λ, pressure difference and average temperature rises.

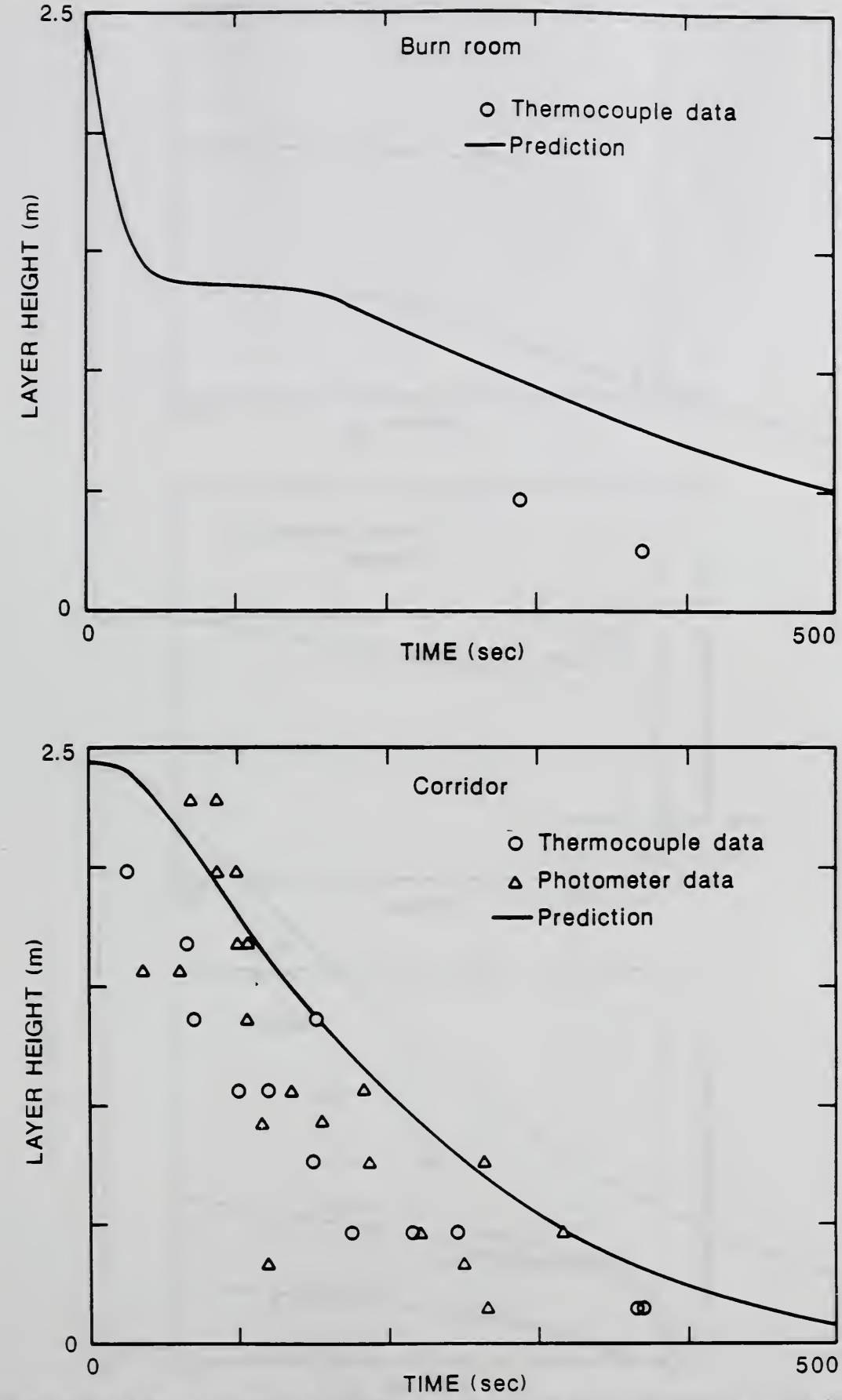

Figure 5a. 25 kW fire, 3/4 Corridor configuration: layer heights.

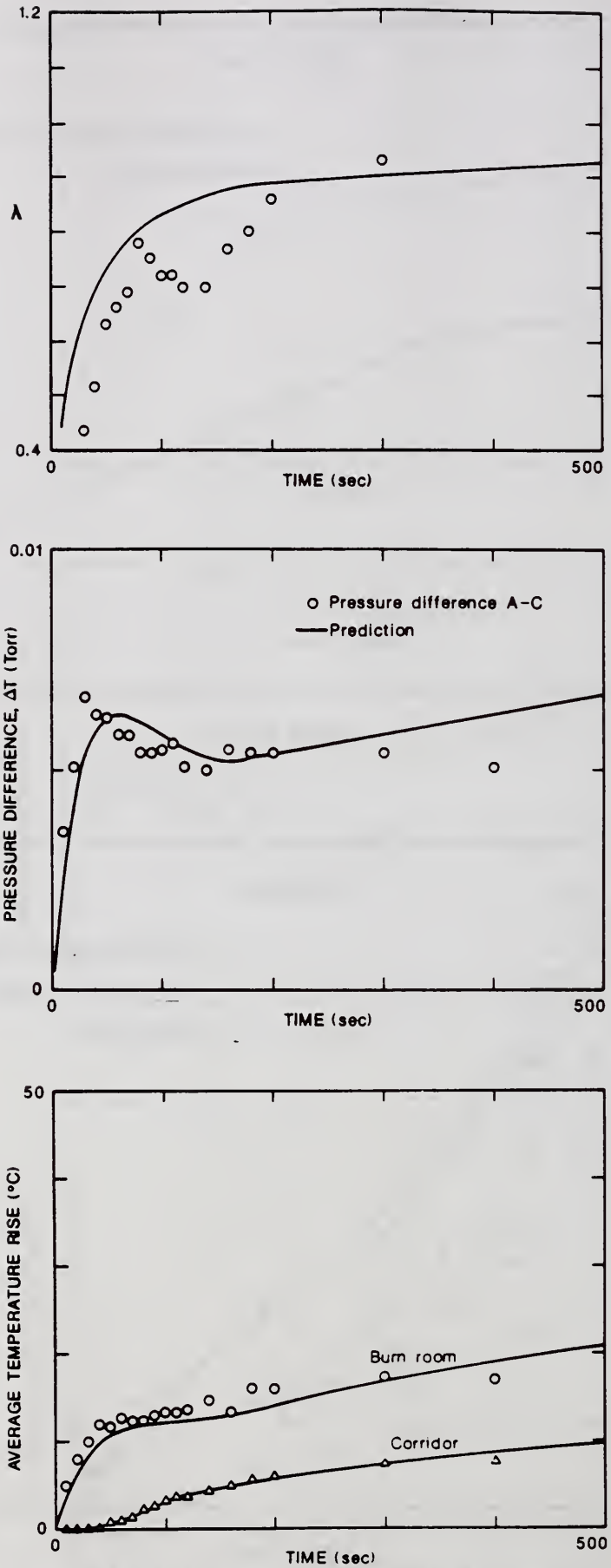

Figure 5b. 25 kW fire, 3/4 Corridor configuration: λ, pressure difference and average temperature rises.

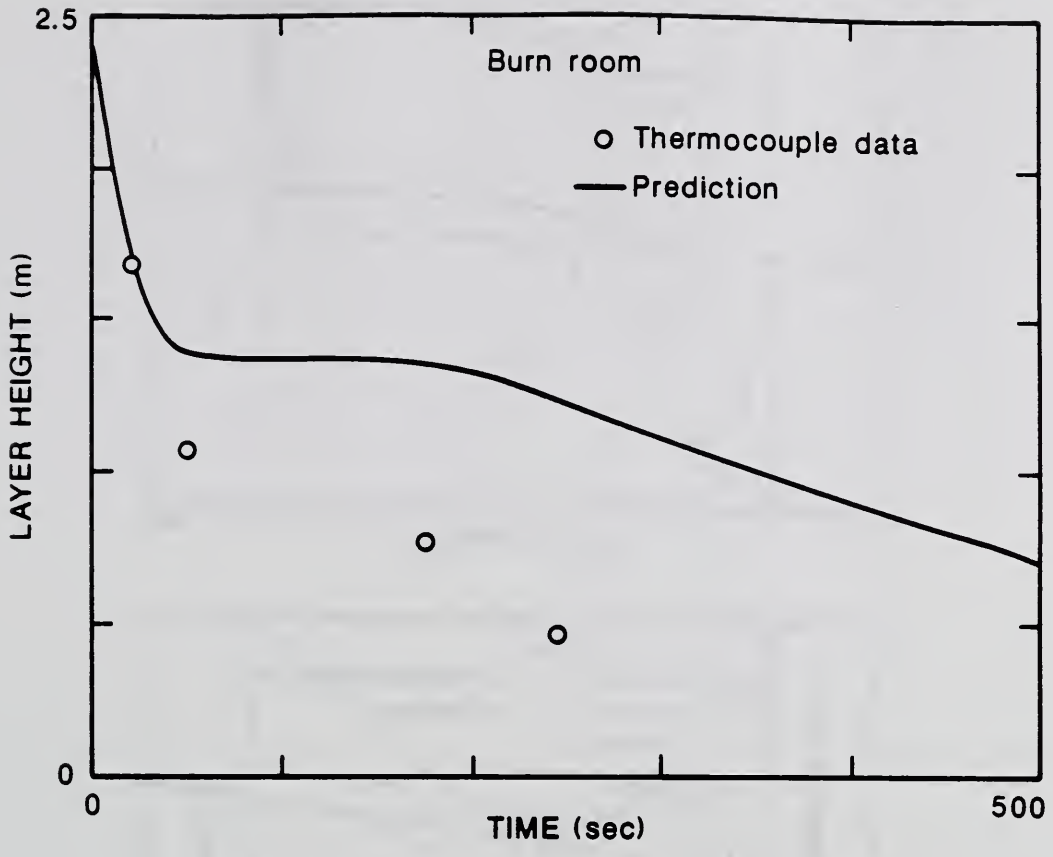

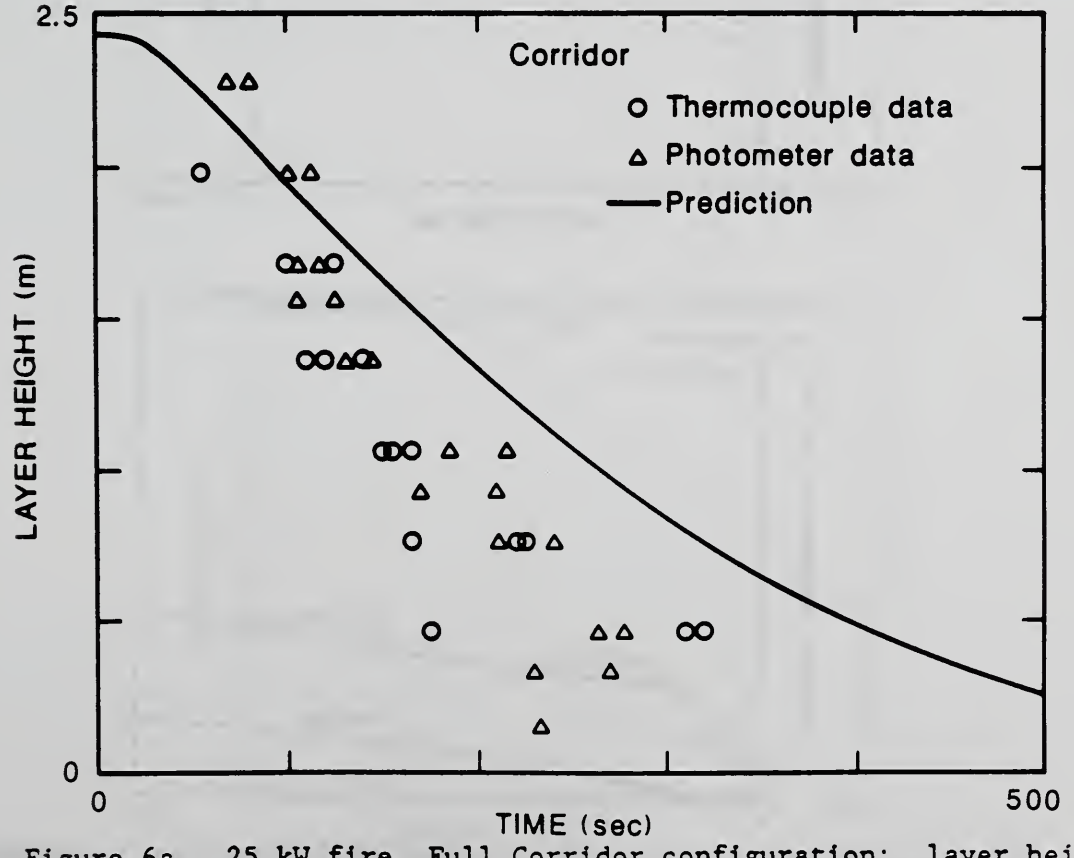

Figure 6a. 25 kW fire, Full Corridor configuration: layer heights.

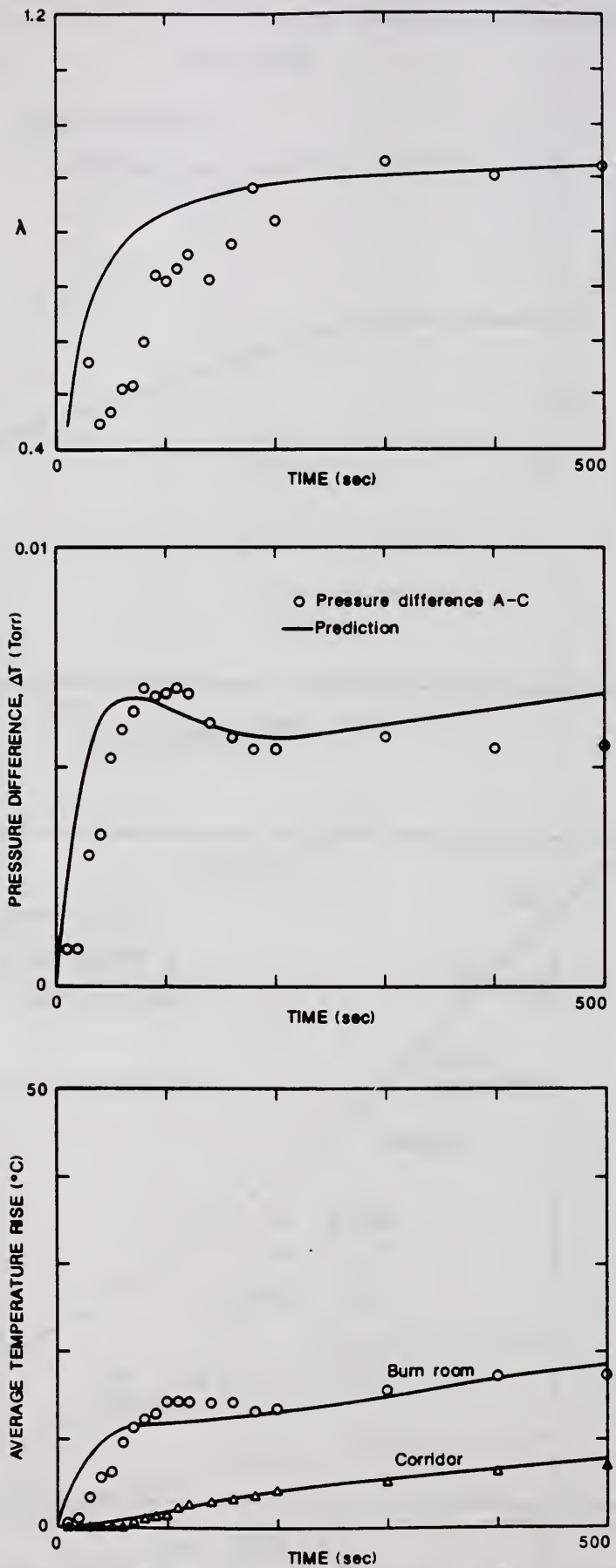

Figure 6b. 25 kW fire, Full Corridor configuration: λ, pressure difference and average temperature rises.

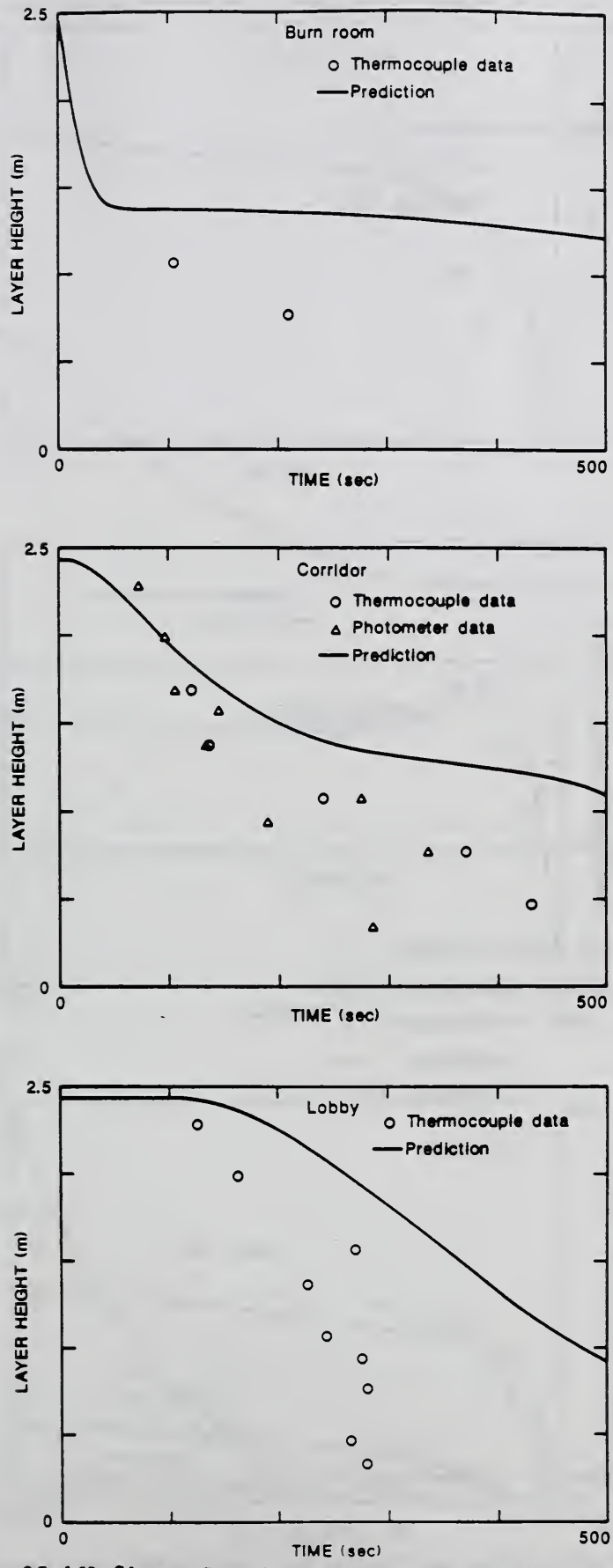

Figure 7a. 25 kW fire, Corridor and Lobby configuration: layer heights

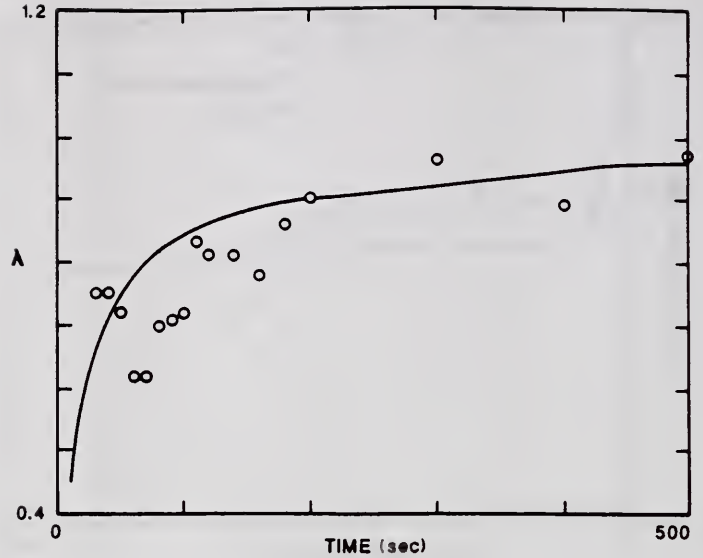

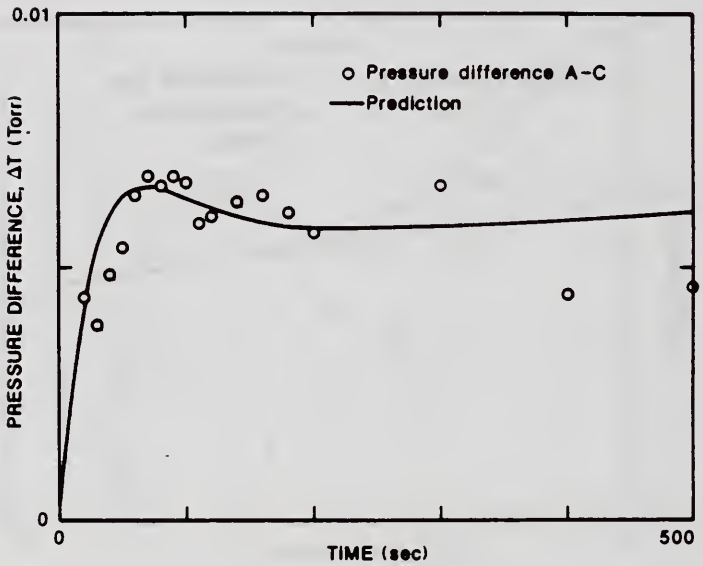

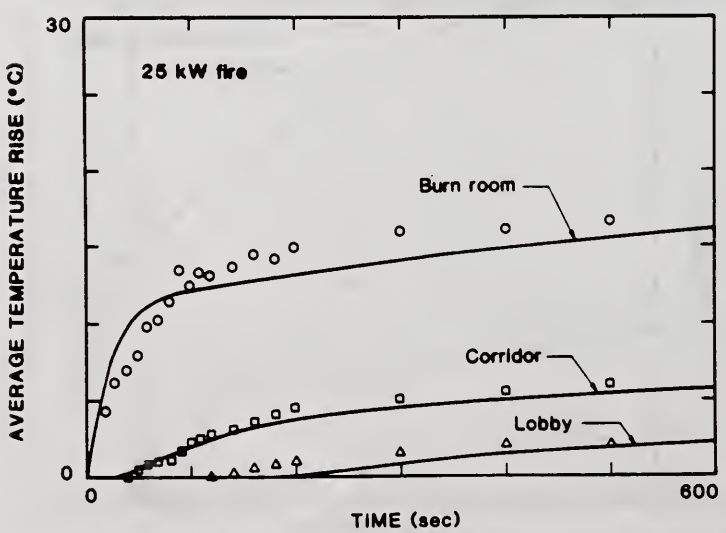

Figure 7b. 25 kW fire, Corridor and Lobby configuration: λ, pressure difference and average temperature rises.

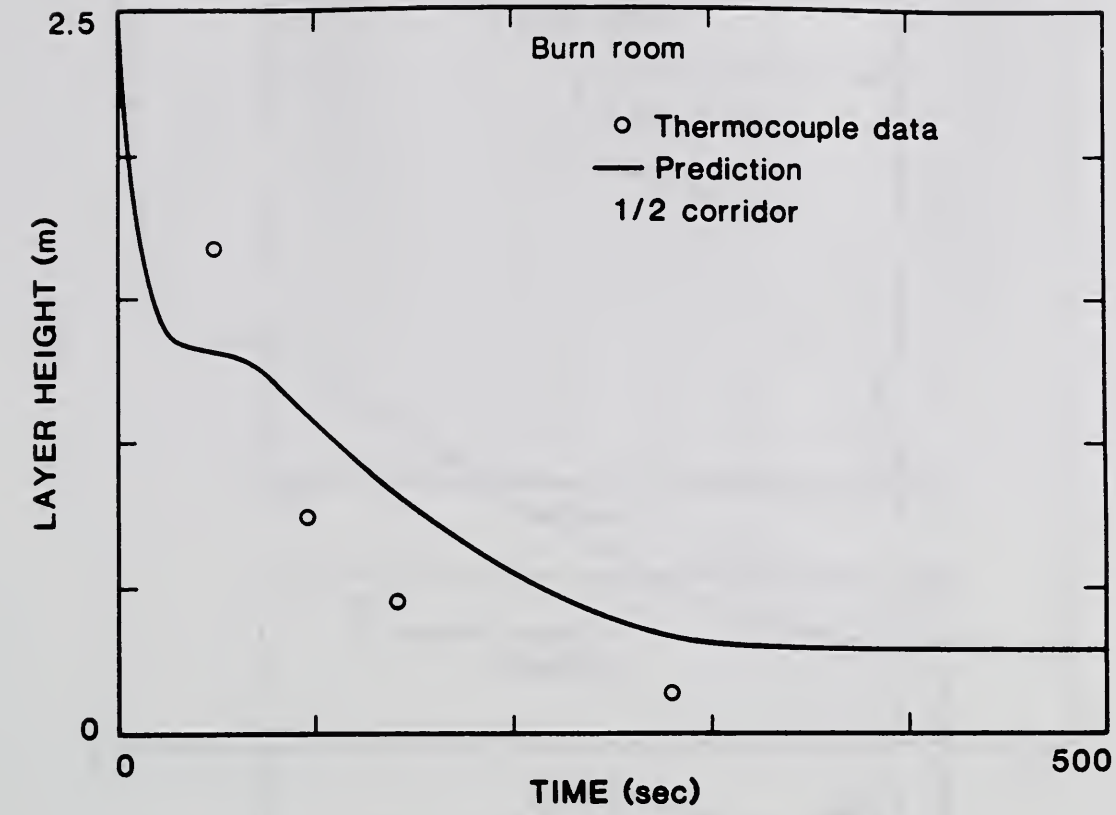

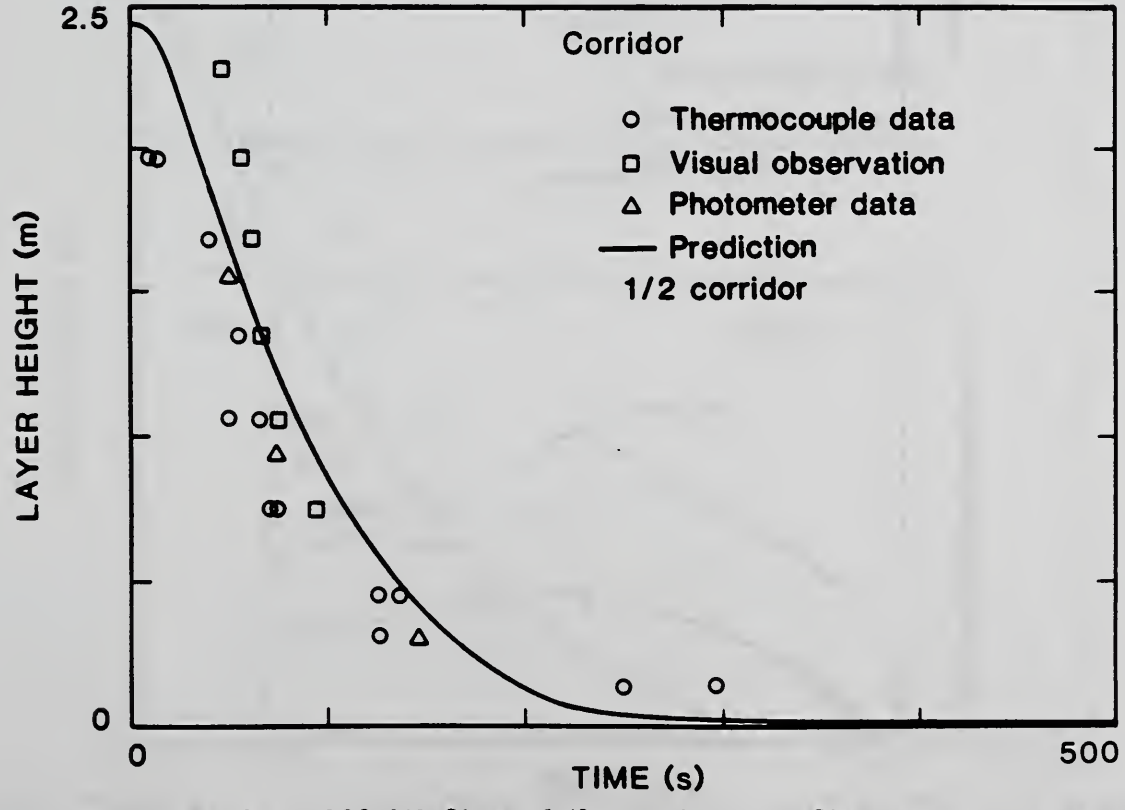

Figure 8a. 100 kW fire, 1/2 Corridor configuration: layer heights

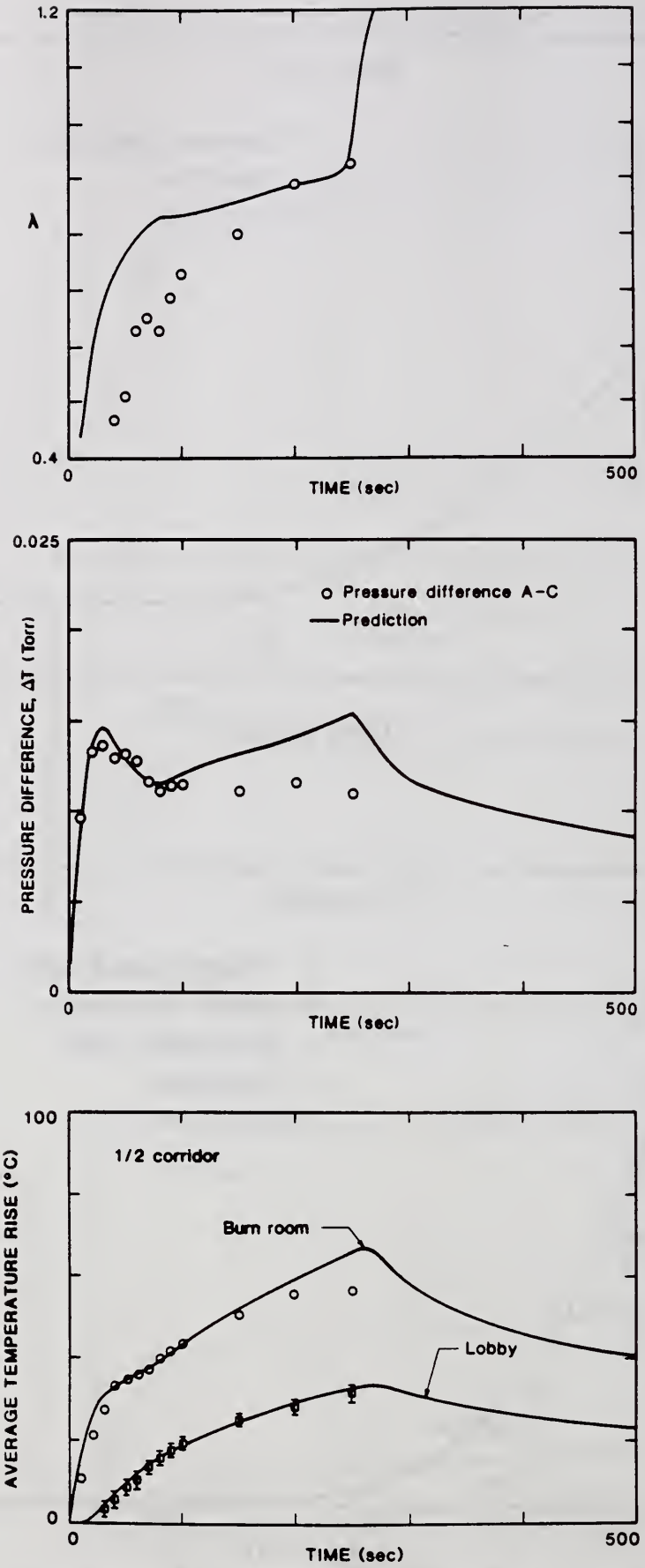

Figure 8b. 100 kW fire, 1/2 Corridor configuration: λ, pressure difference and average temperature rises.

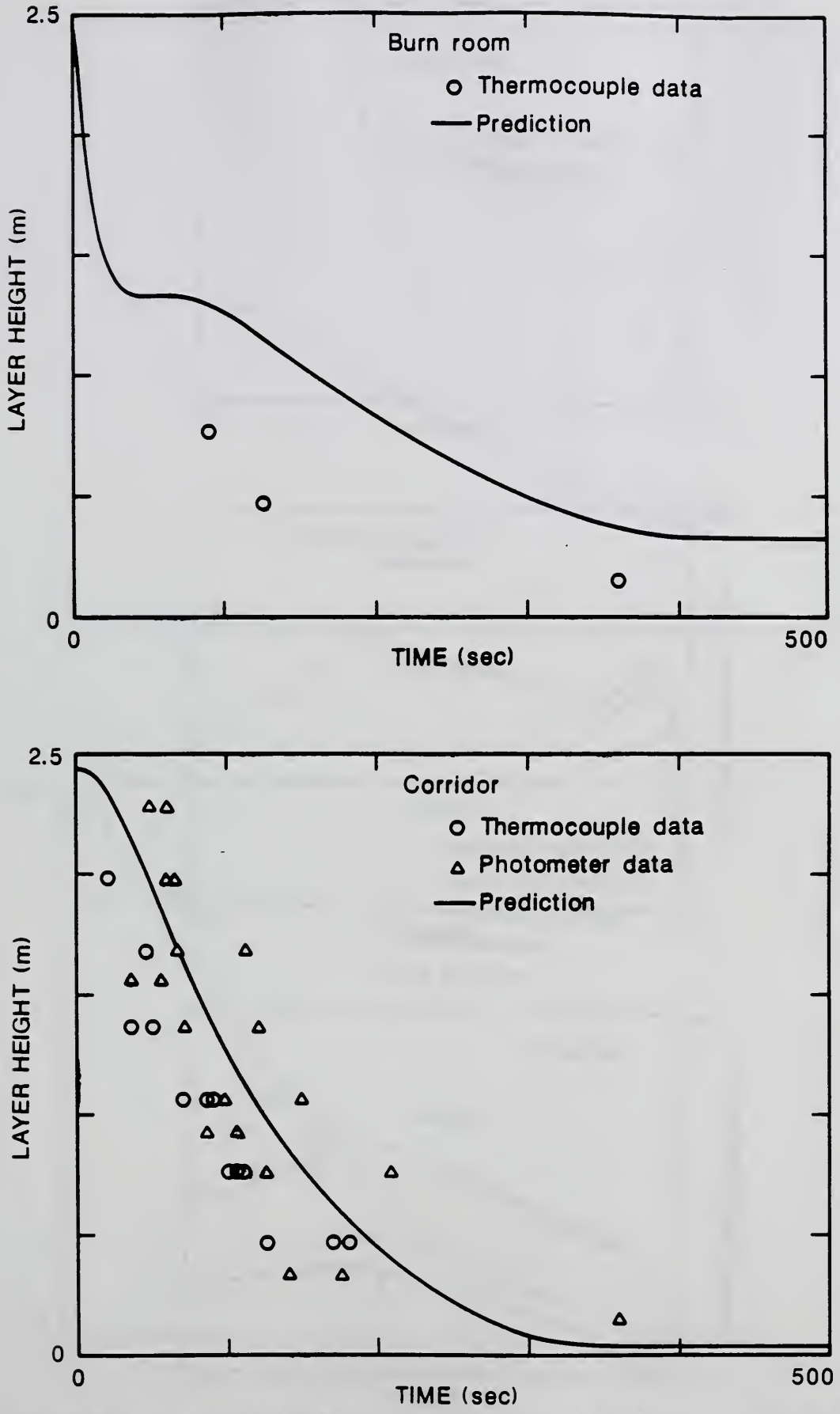

Figure 9a. 100 kW fire, 3/4 Corridor configuration: layer heights.

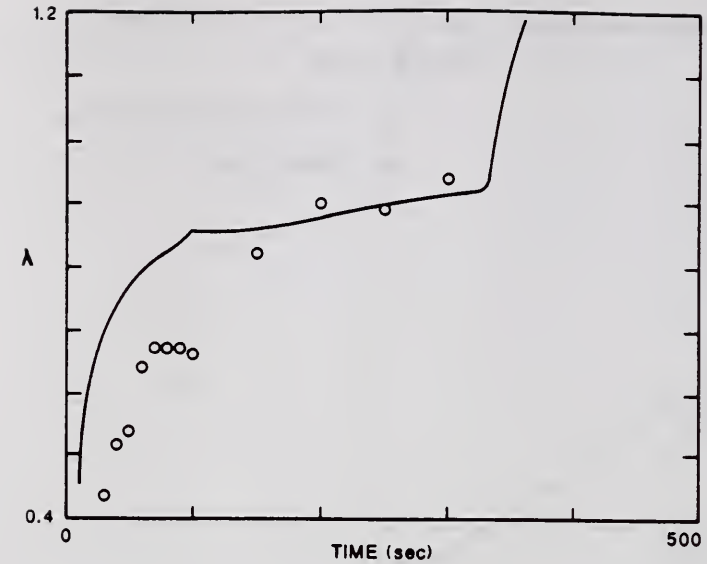

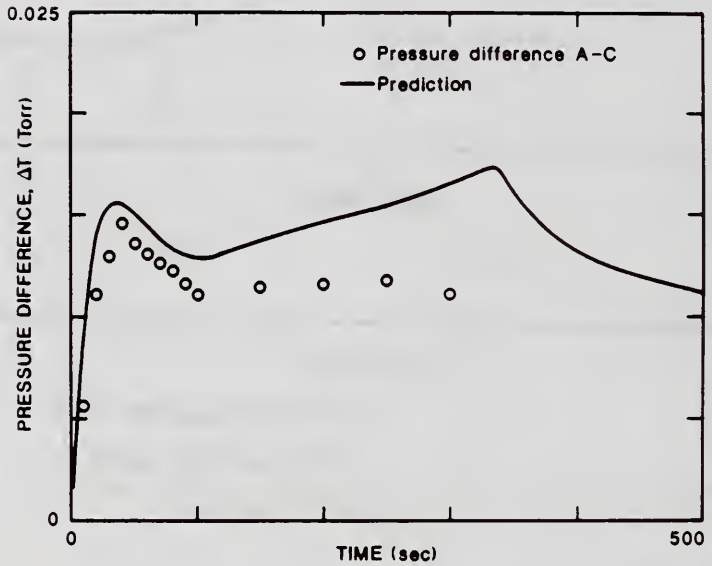

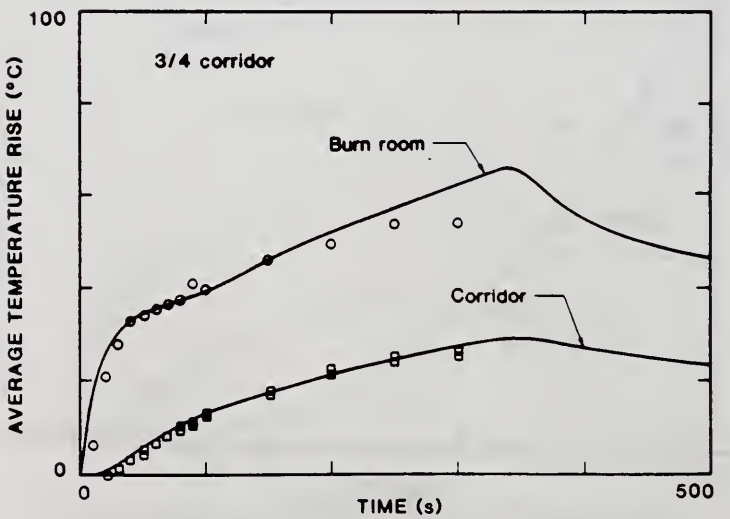

Figure 9b. 100 kW fire, 3/4 Corridor configuration: λ, pressure difference and average temperature rises.

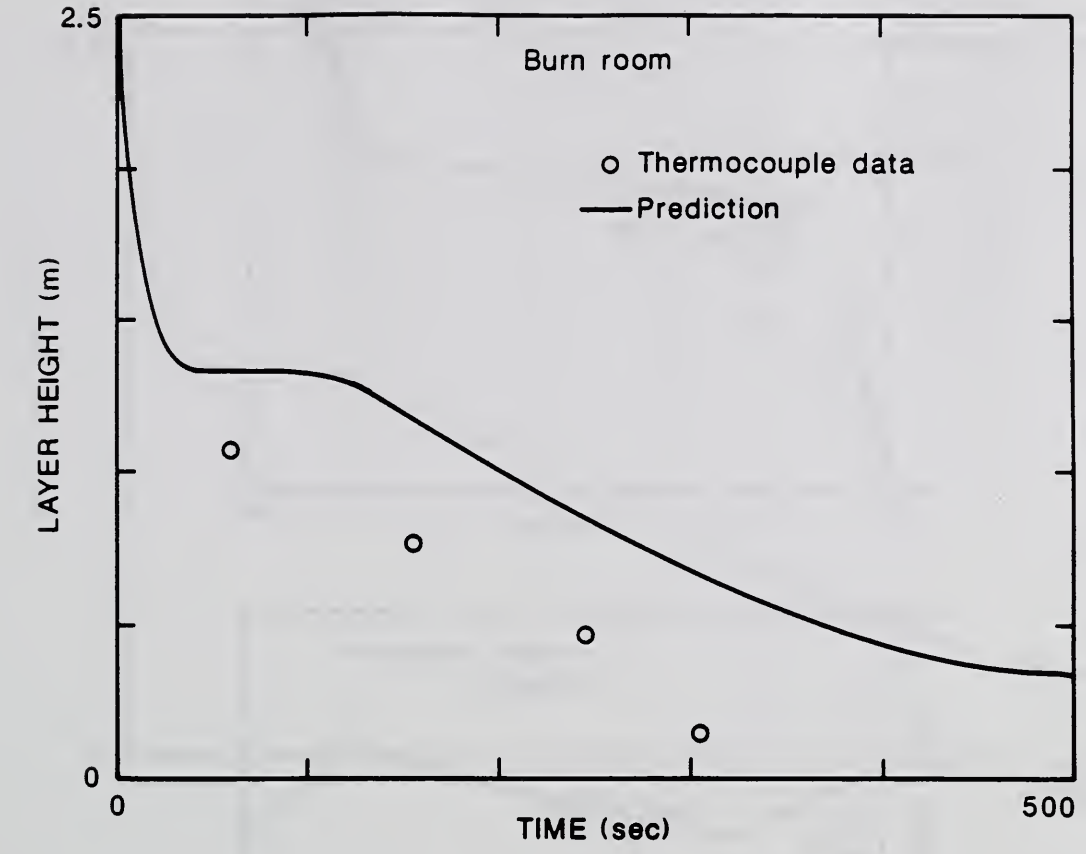

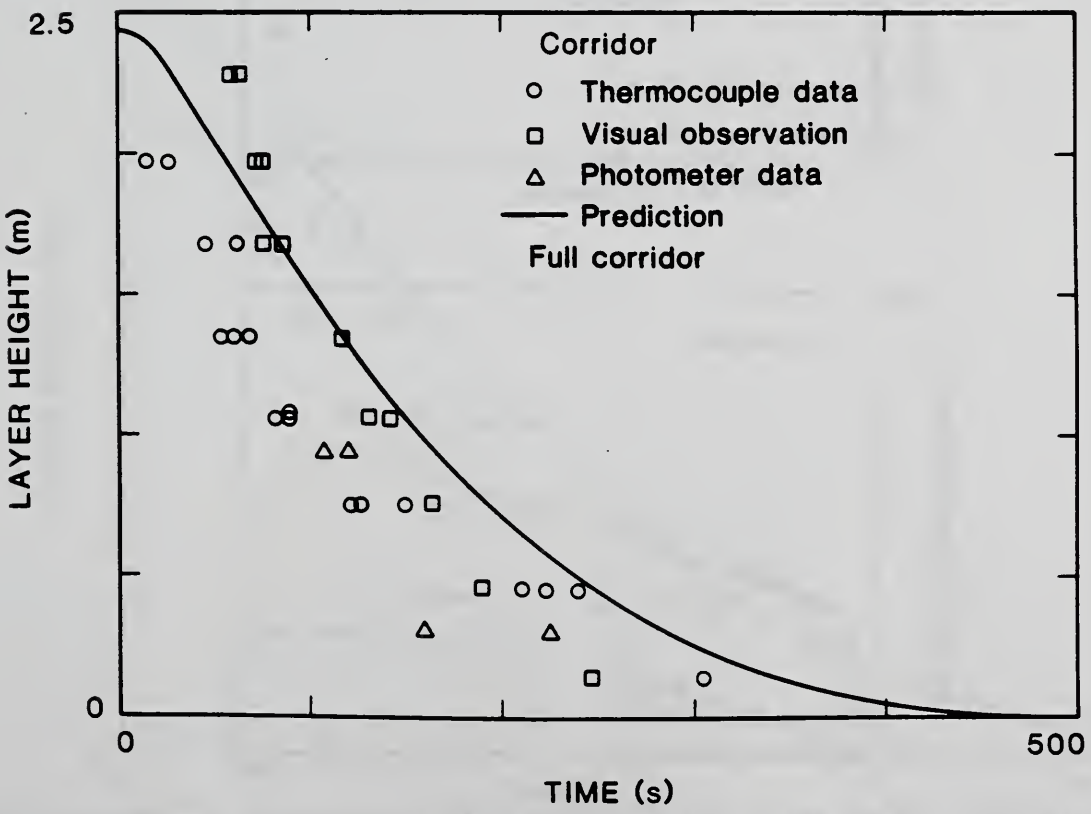

Figure 10a. 100 kW fire, Full Corridor configuration: layer heights.

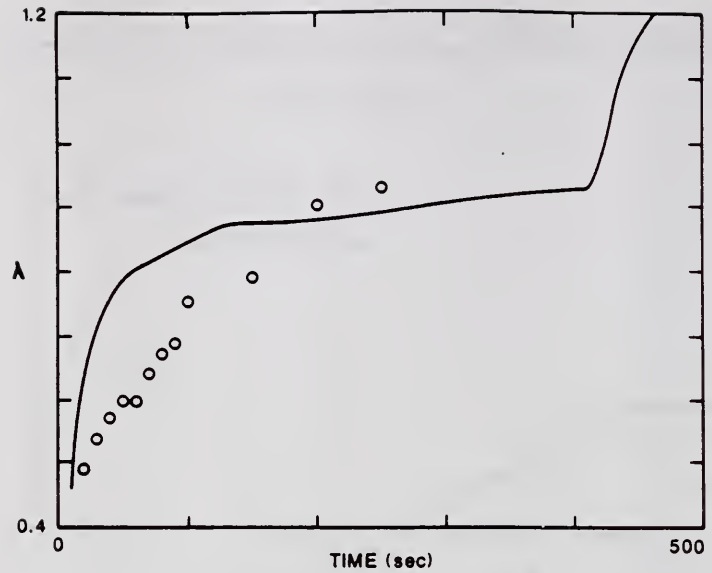

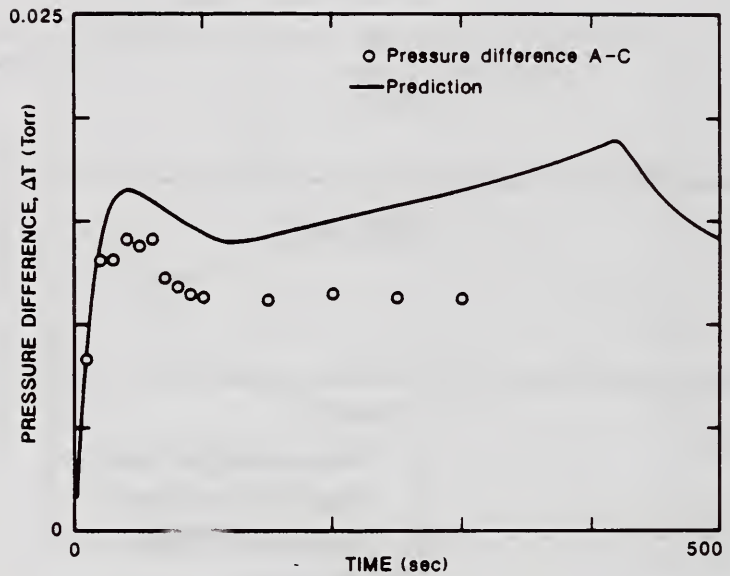

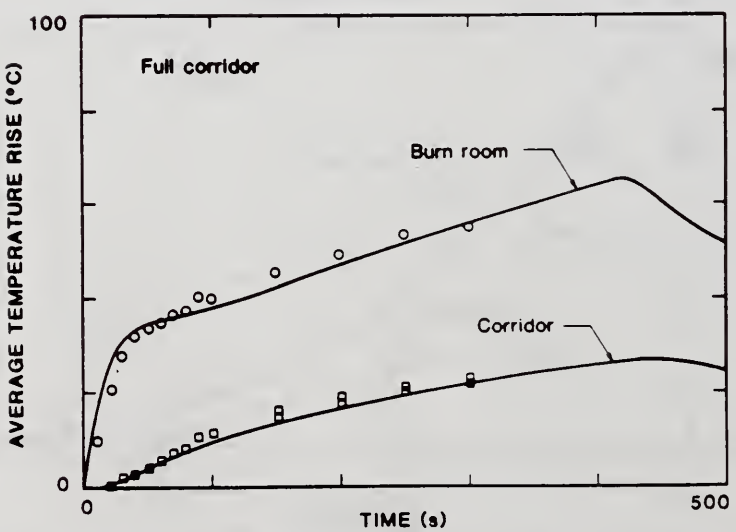

Figure 10b. 100 kW fire, Full Corridor configuration: λ, pressure difference and average temperature rises.

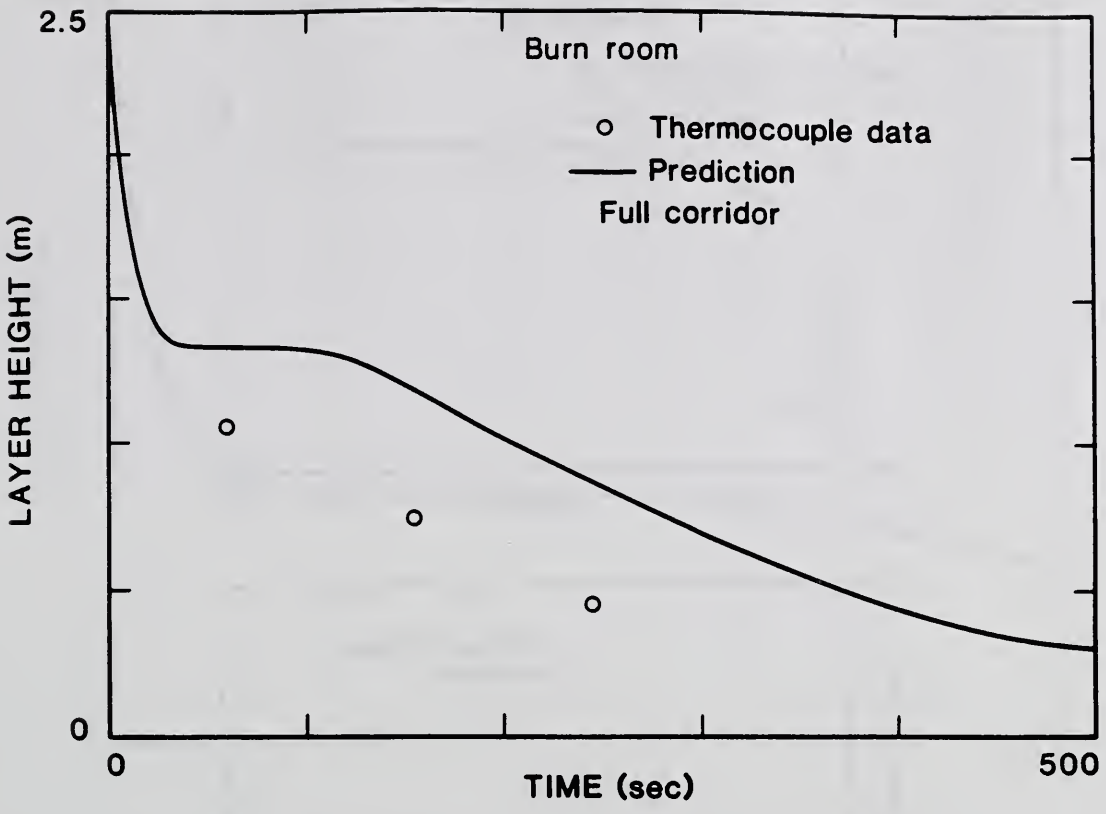

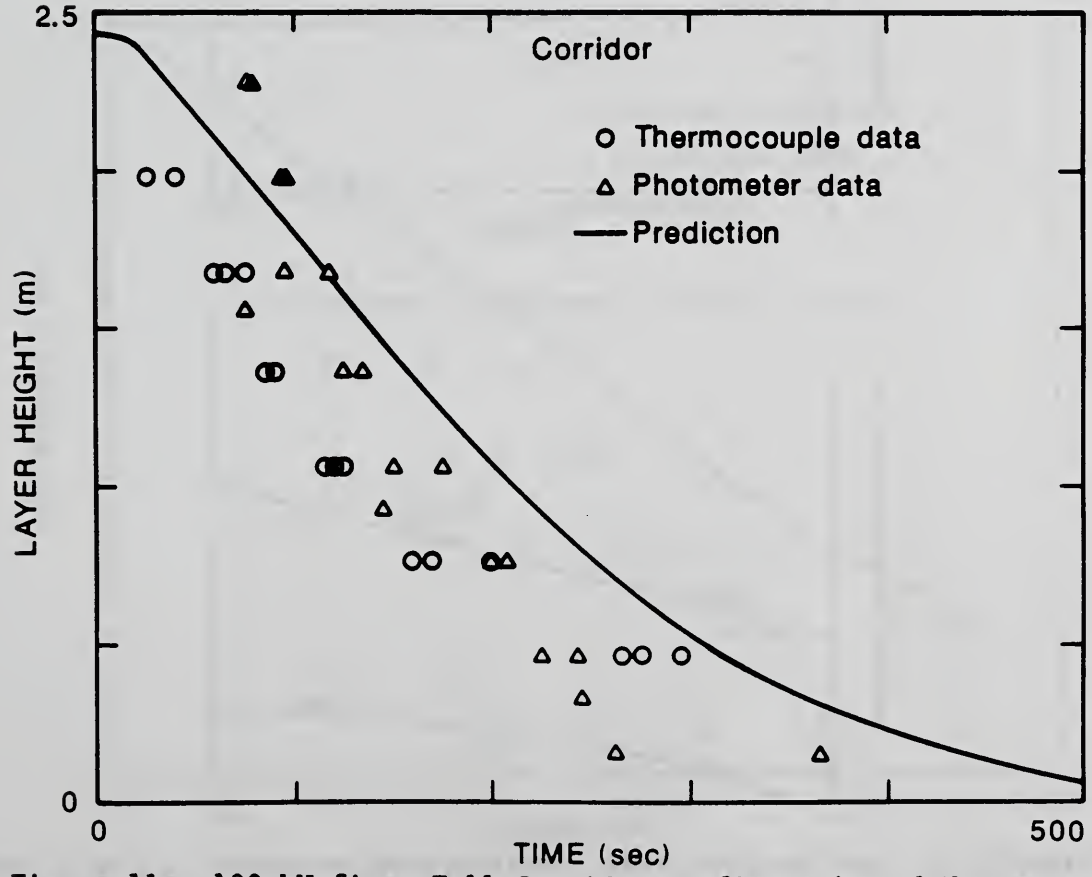

Figure 11a. 100 kW fire, Full Corridor configuration, 1/2 width door burn room to corridor: layer heights.

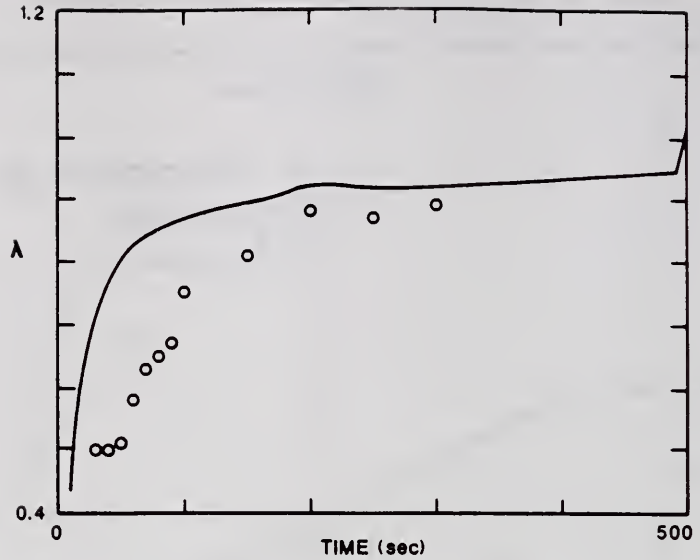

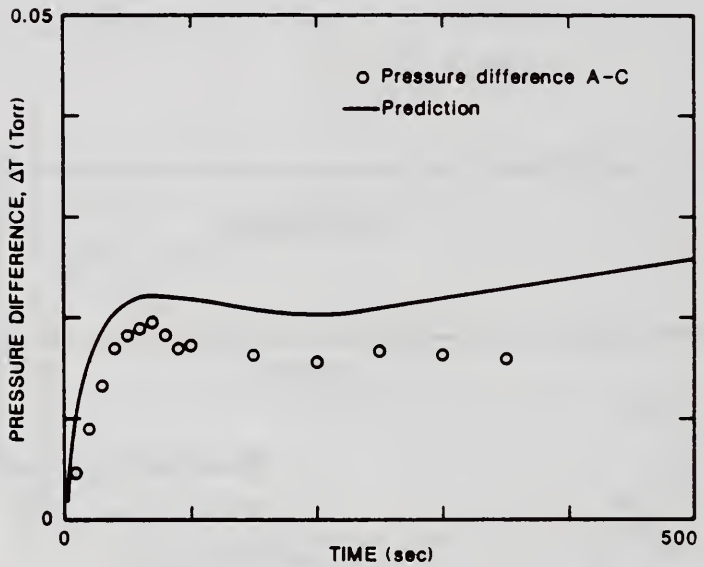

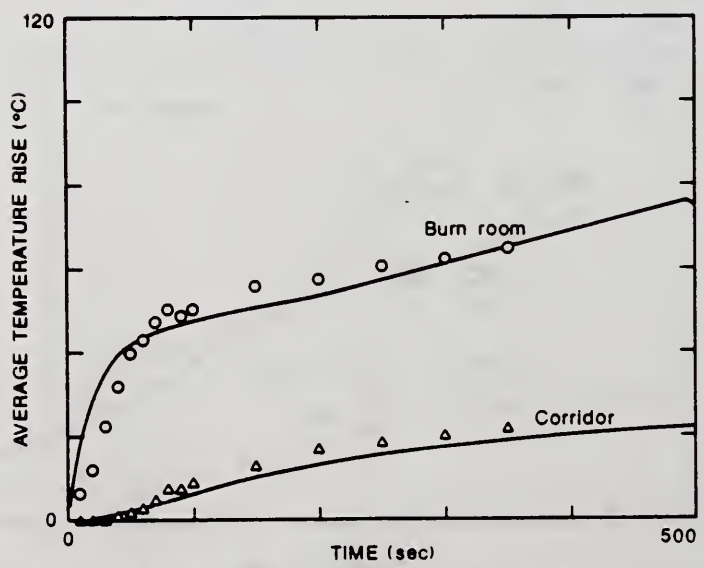

Figure 11b. 100 kW fire, Full Corridor configuration, 1/2 width door burn room to corridor: λ, pressure difference and average temperature rises.

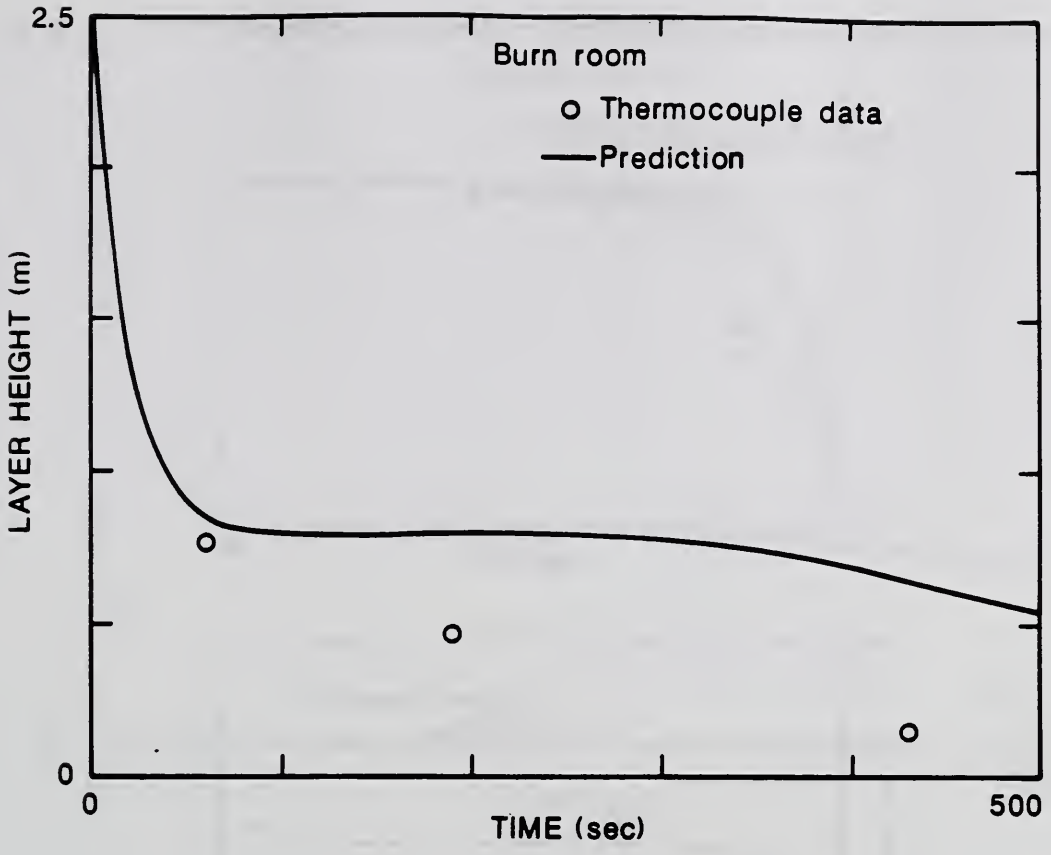

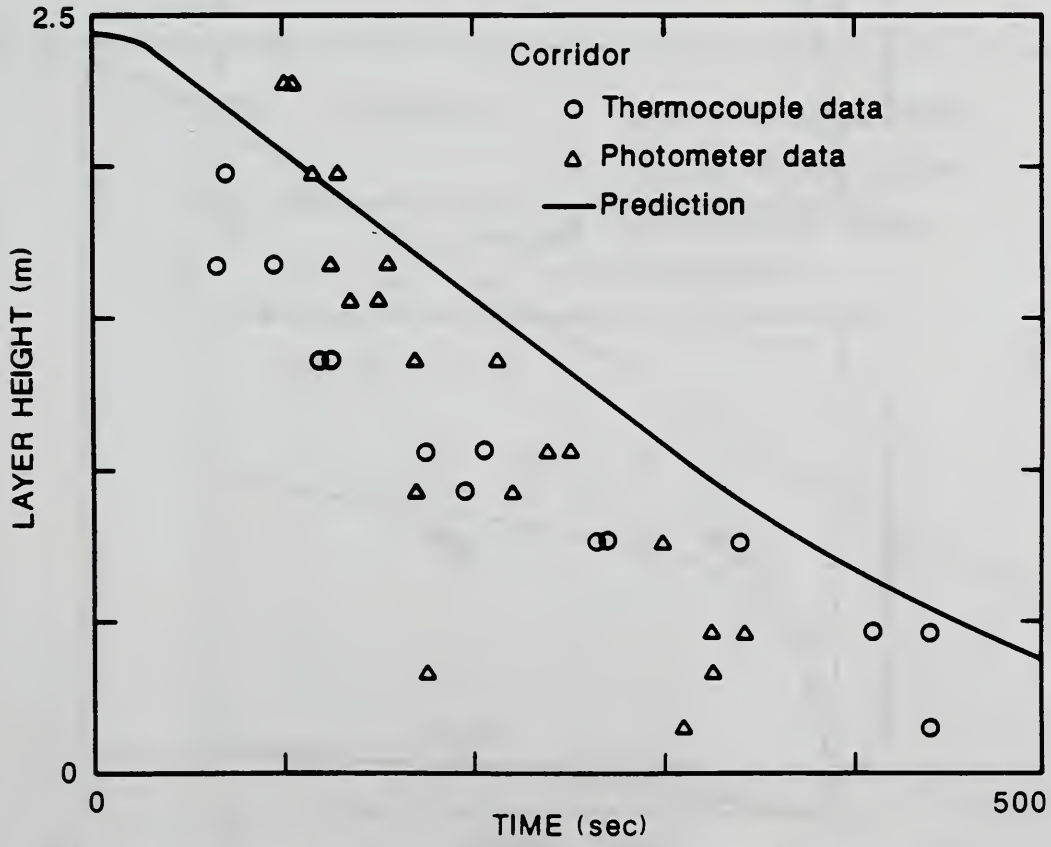

Figure 12a. 100 kW fire, Full Corridor configuration, 1\4 width door burn room to corridor: layer heights.

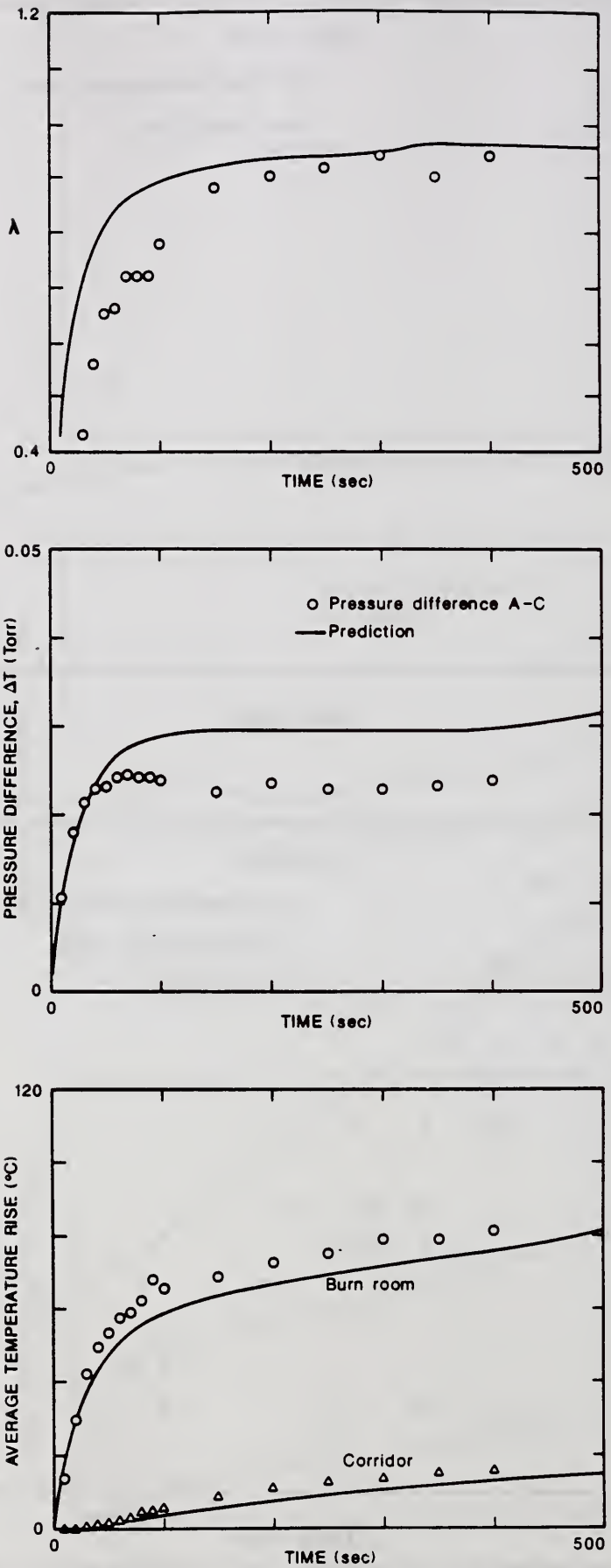

Figure 12b. 100 kW fire, Full Corridor configuration, 1\4 width door burn room to corridor: λ, pressure difference and average temperature rises.

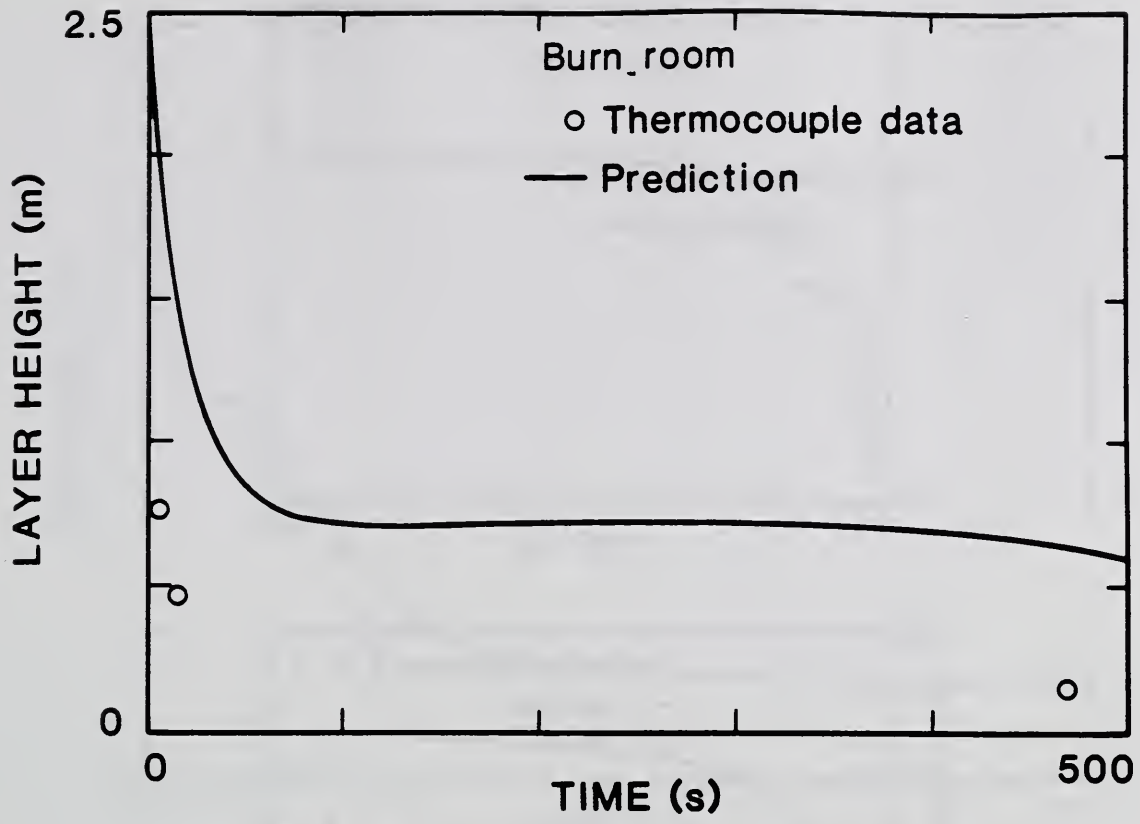

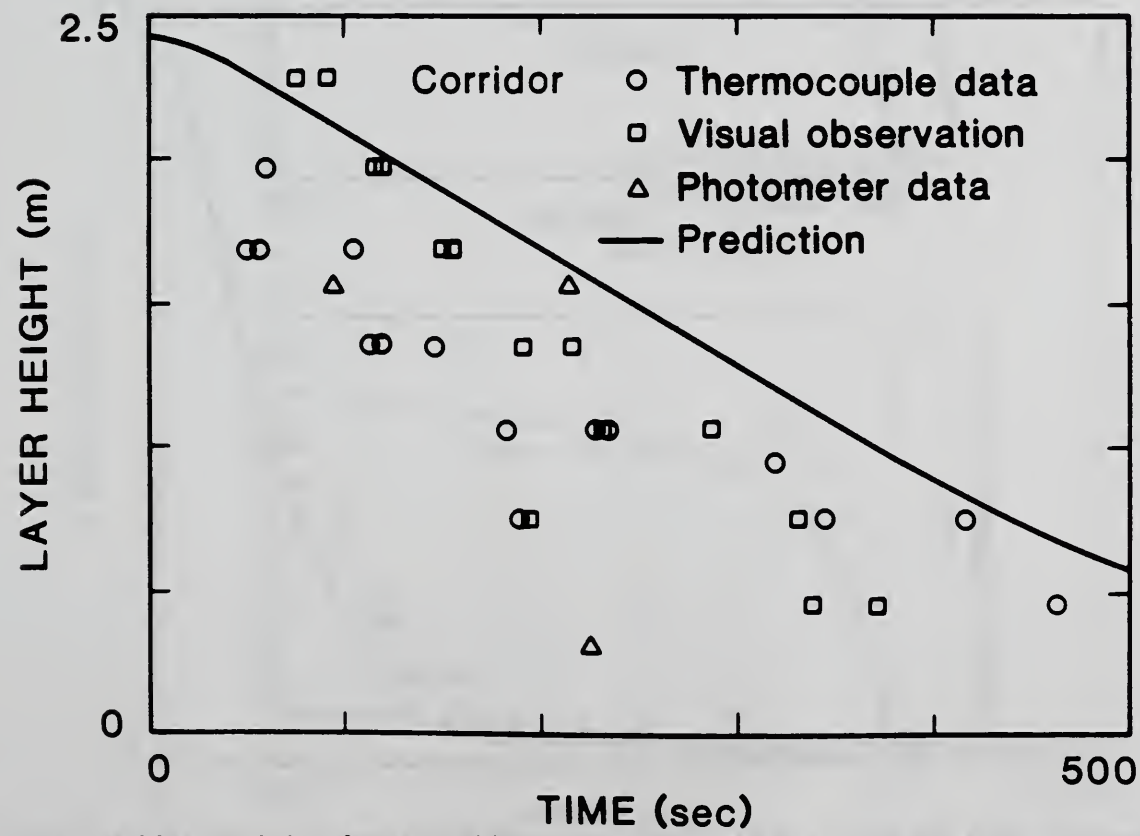

Figure 13a. 100 kW fire, Full Corridor configuration, 1/8 width door burn room to corridor: layer heights.

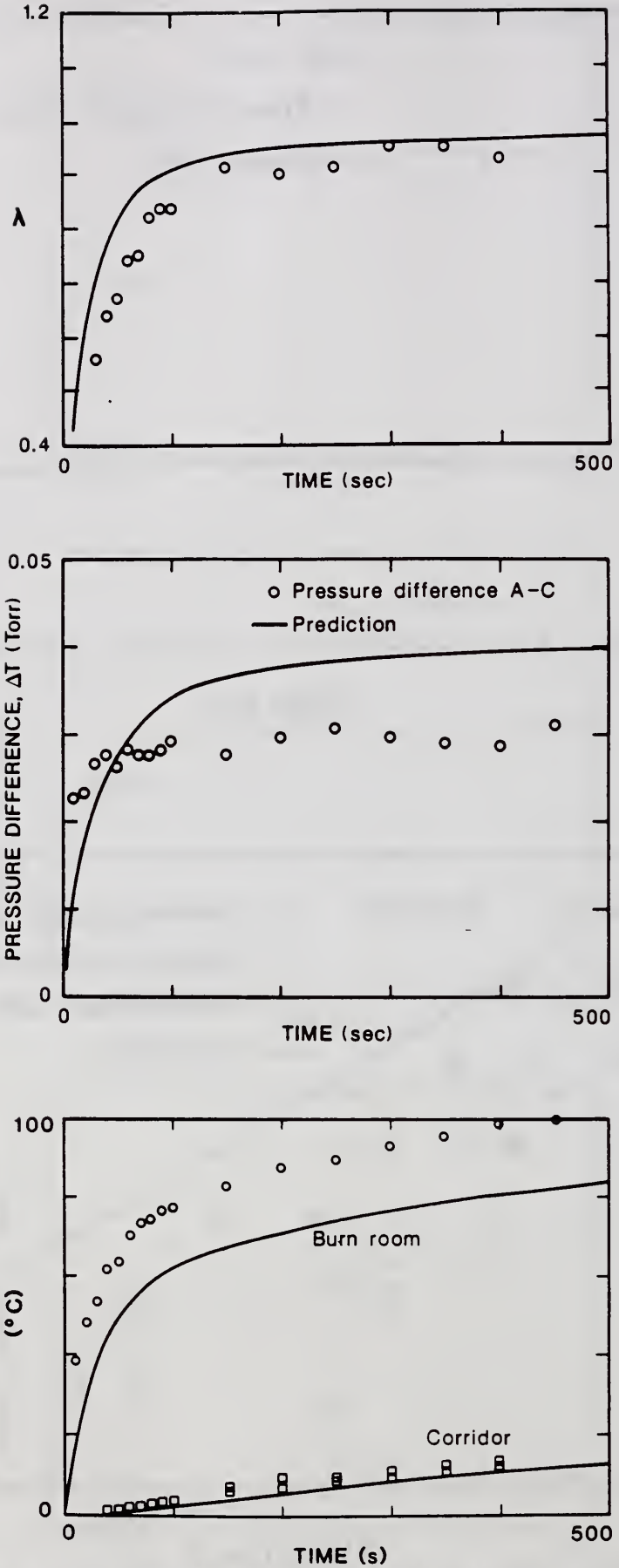

Figure 13b. 100 kW fire, Full Corridor configuration, 1/8 width door burn room to corridor: λ, pressure difference and average temperature rises.

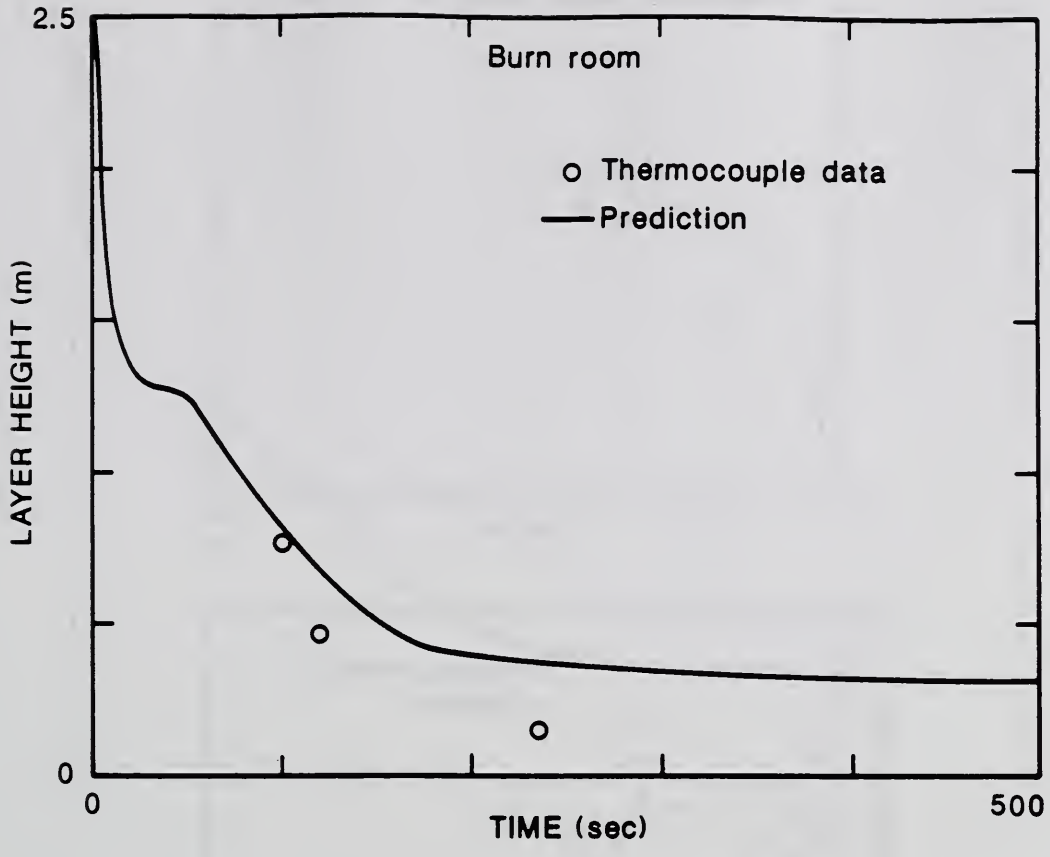

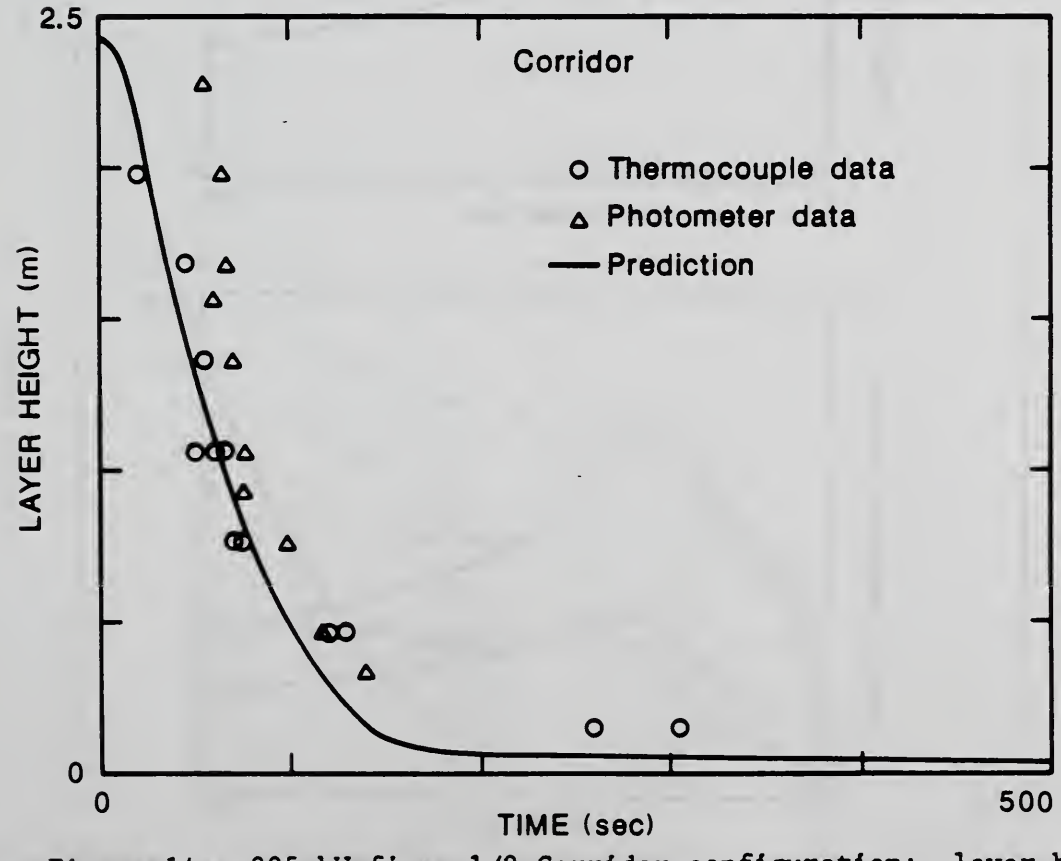

Figure 14a. 225 kW fire, 1/2 Corridor configuration: layer heights.

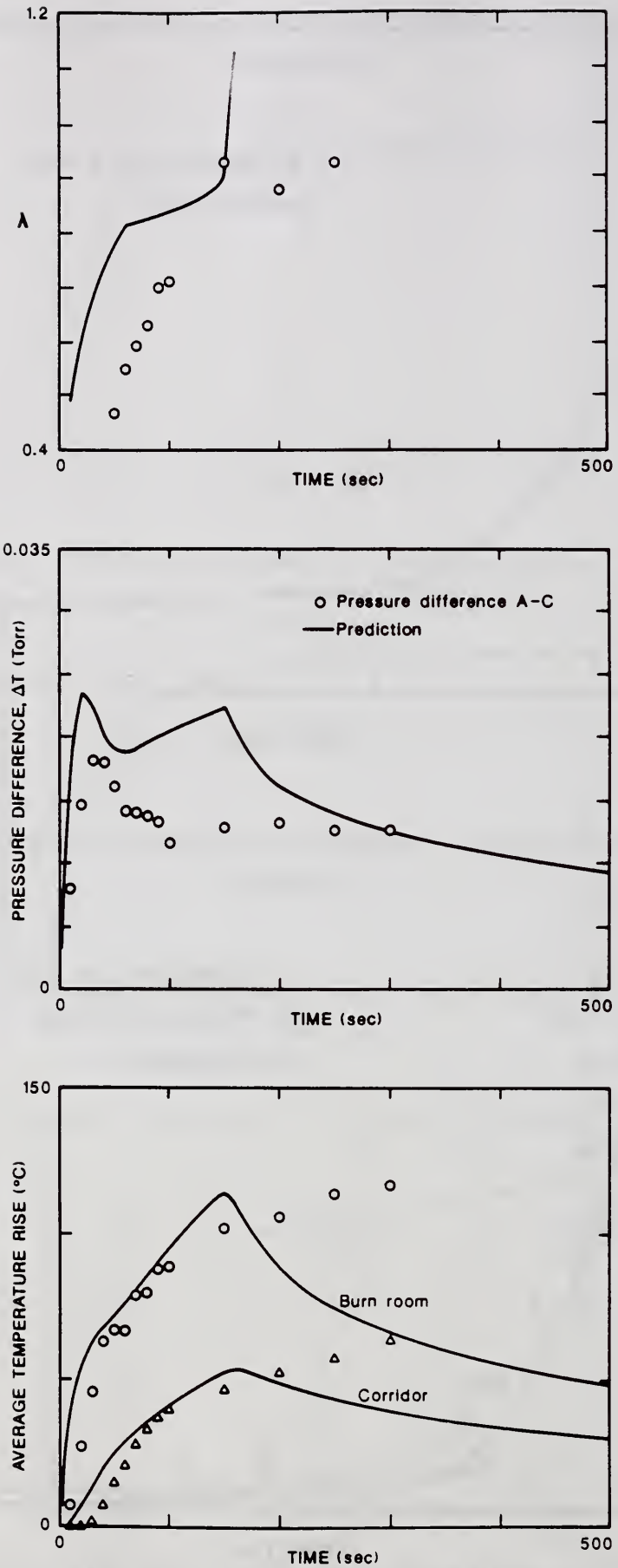

Figure 14b. 225 kW fire, 1/2 Corridor configuration: λ, pressure difference and average temperature rises.

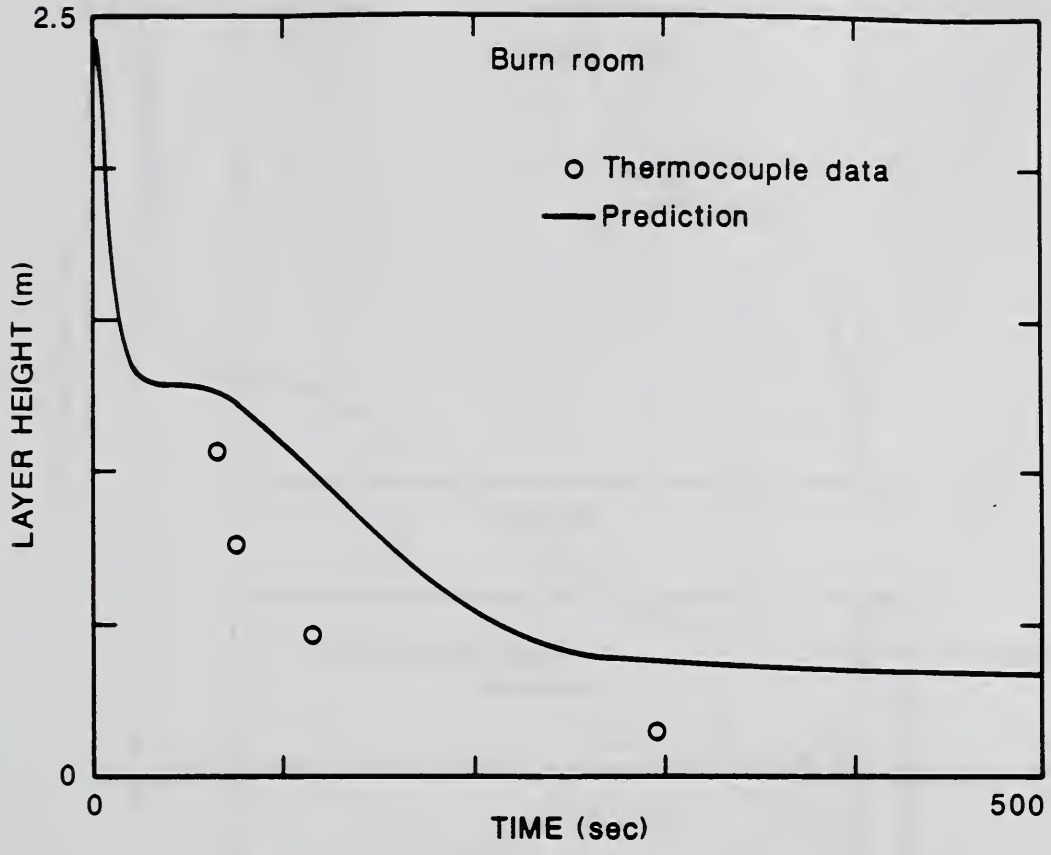

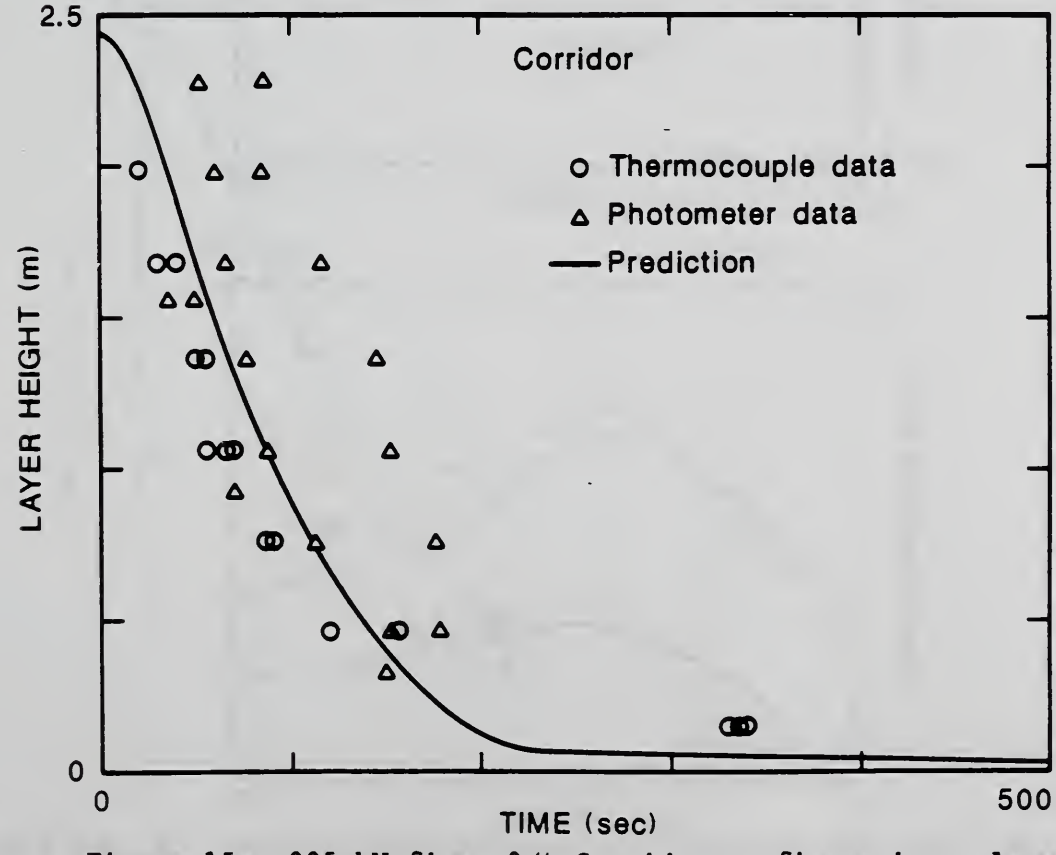

Figure 15a. 225 kW fire, 3/4 Corridor configuration: layer heights.

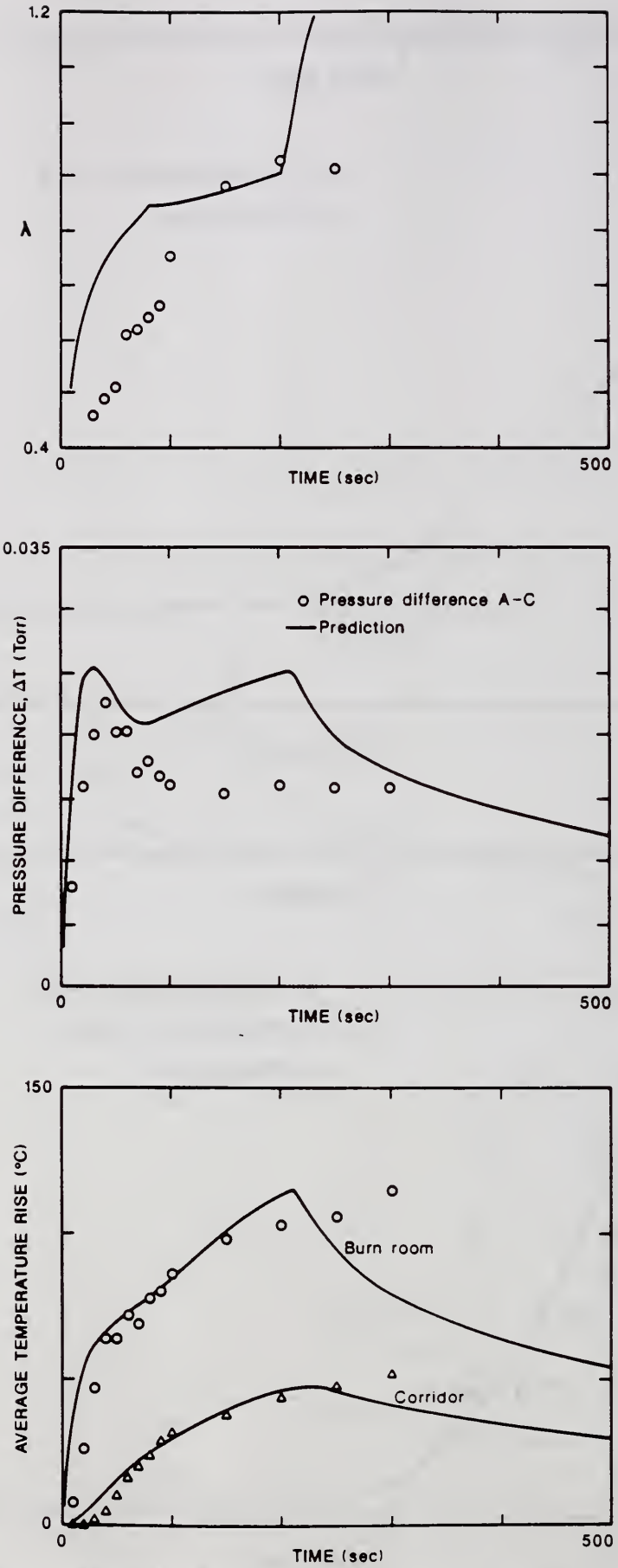

Figure 15b. 225 kW fire, 3/4 Corridor configuration: λ, and average temperature rises.

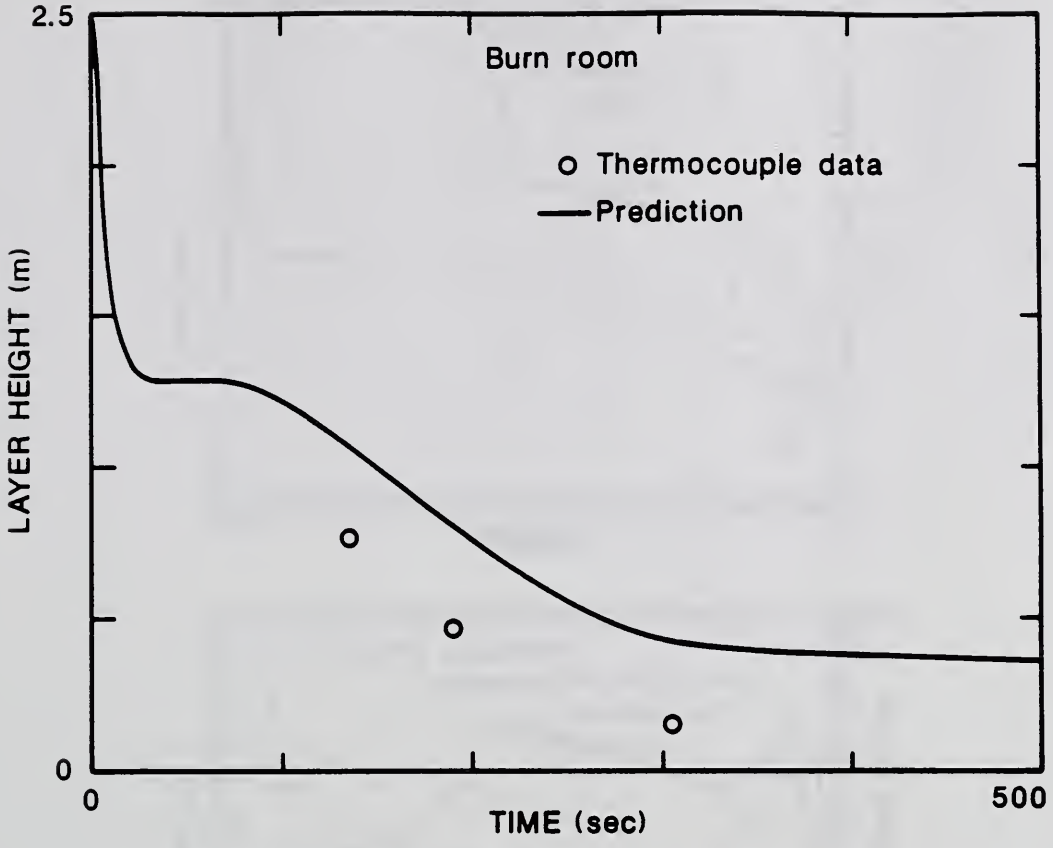

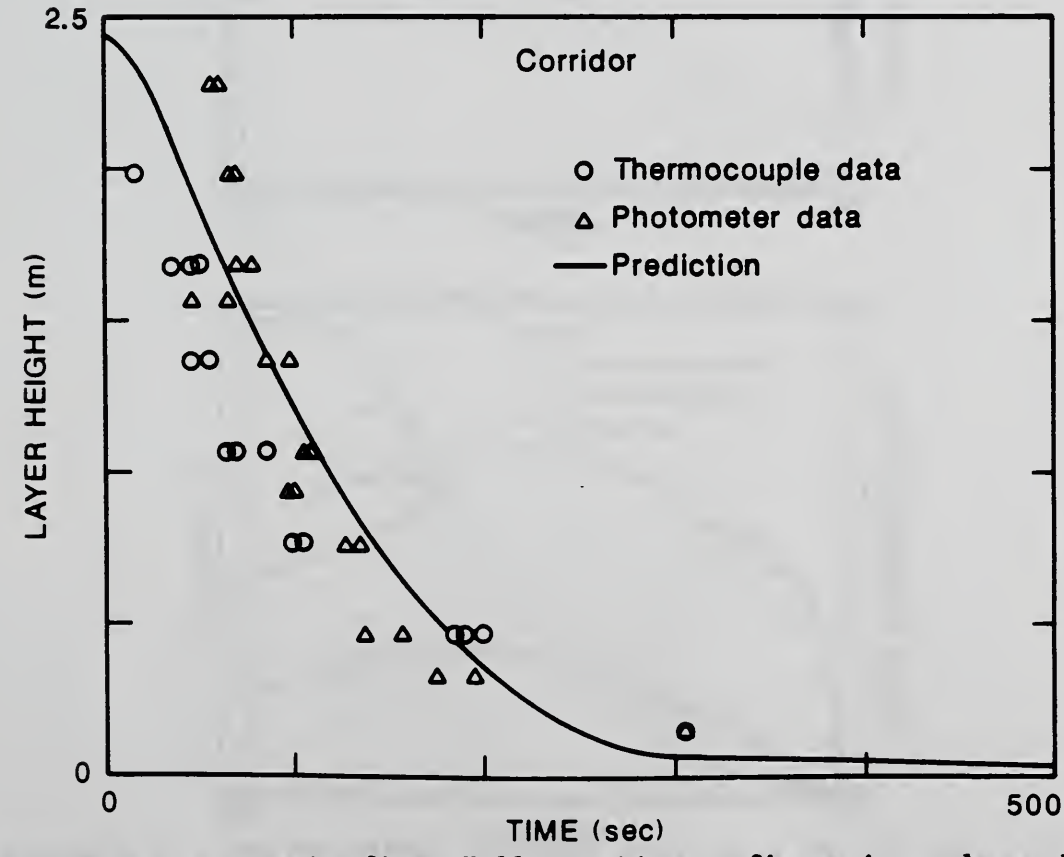

Figure 16a. 225 kW fire, Full Corridor configuration: layer heights.

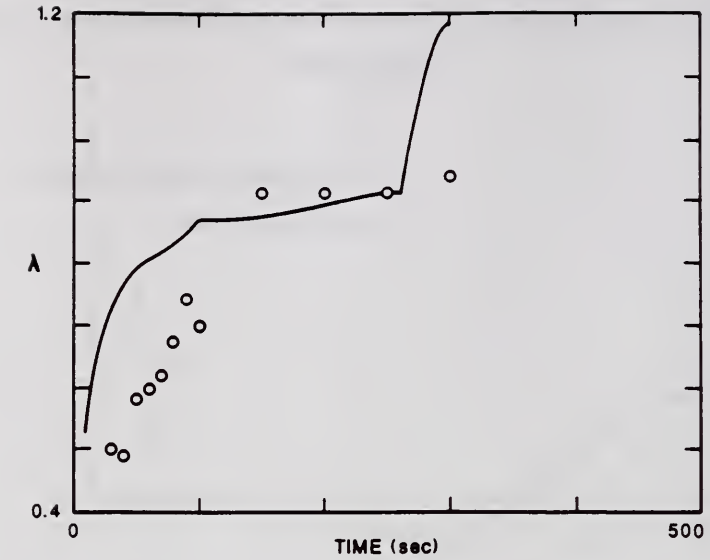

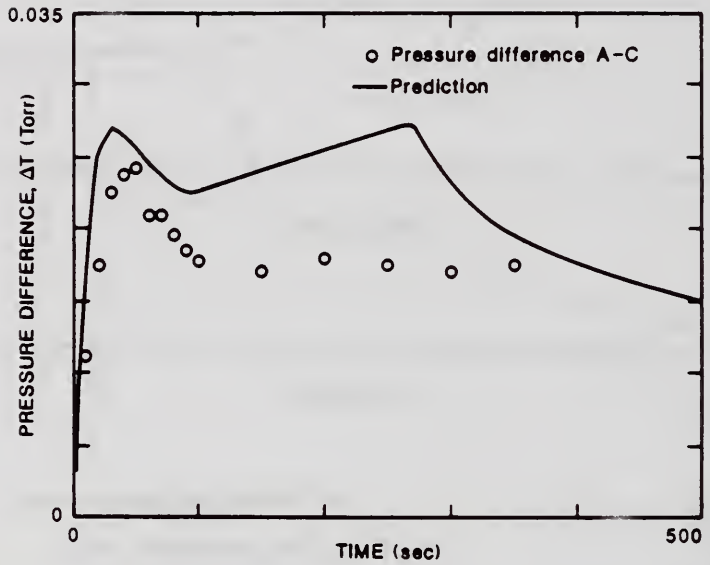

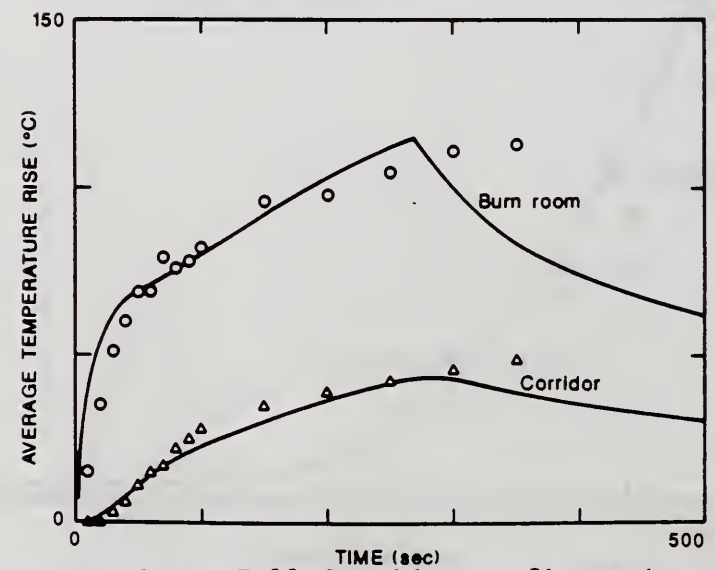

Figure 16b. 225 kW fire, Full Corridor configuration: λ, pressure difference and average temperature rises.

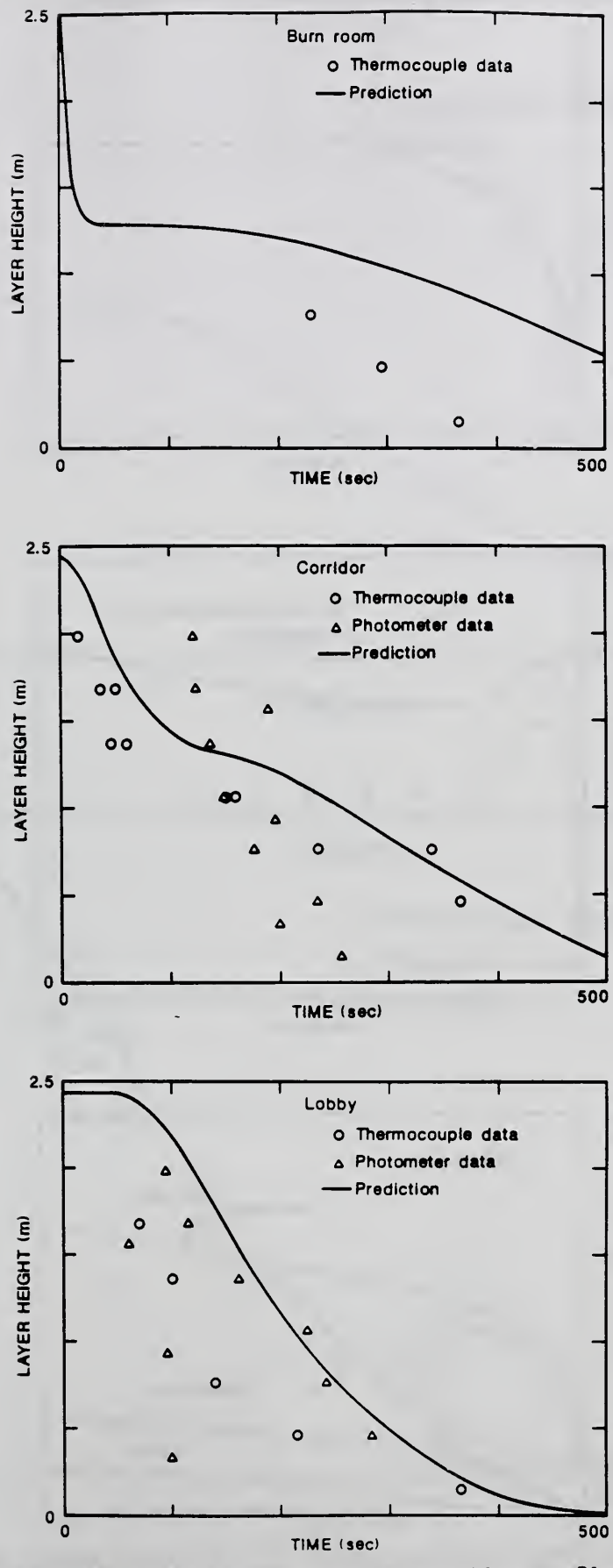

Figure 17a. 225 kW fire, Corridor and Lobby configuration: layer heig

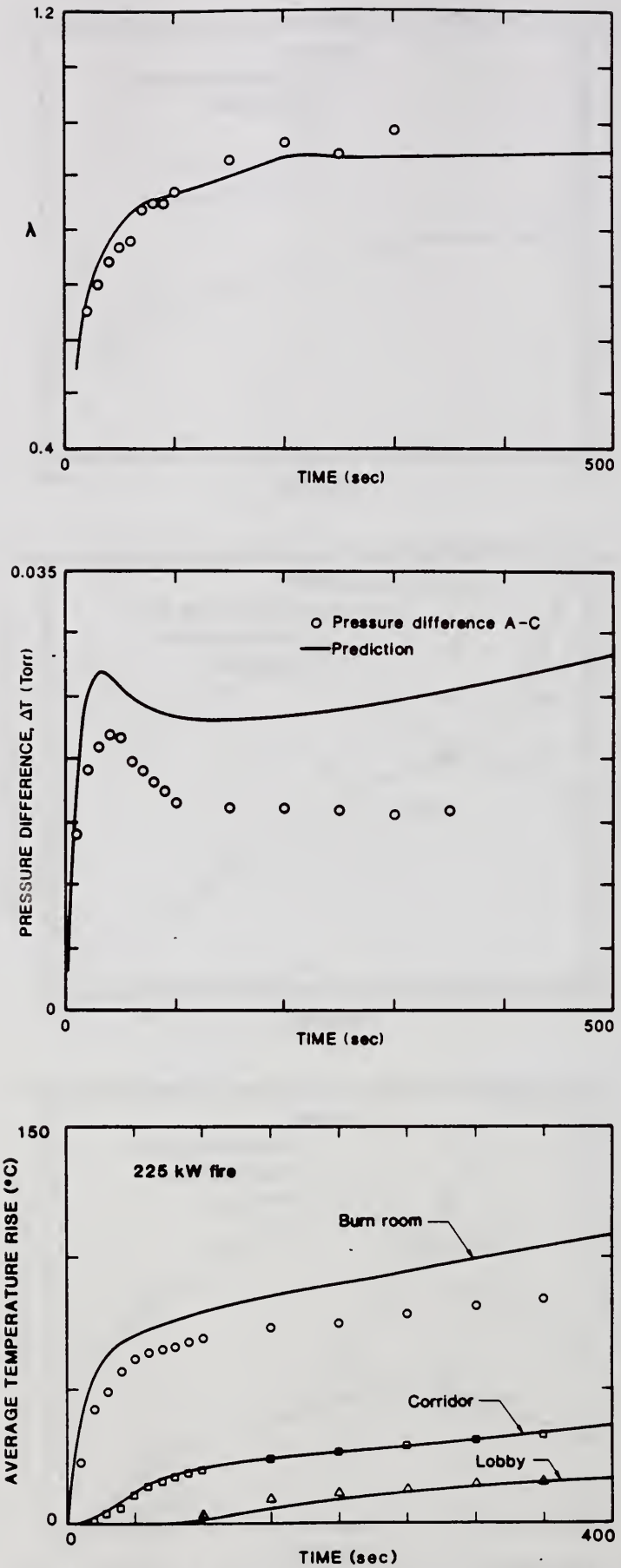

Figure 17b. 225 kW fire, Corridor and Lobby configuration: λ, pressure difference and average temperature rises.

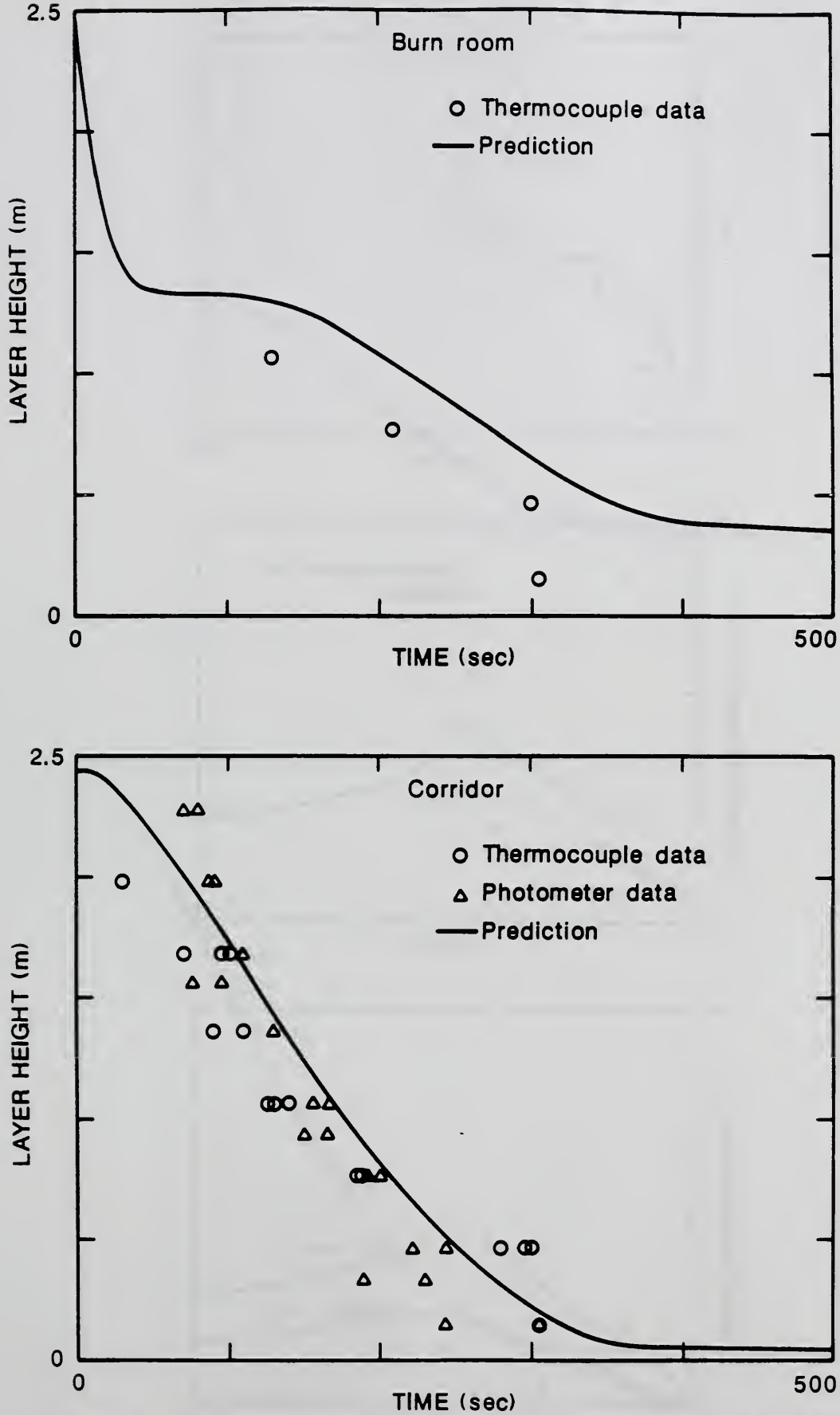

Figure 18a. Ramp fire, 1/2 Corridor configuration: layer heights.

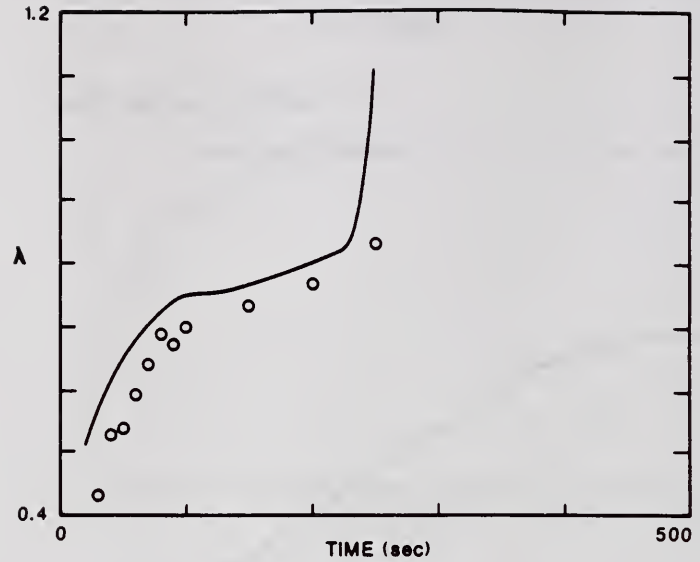

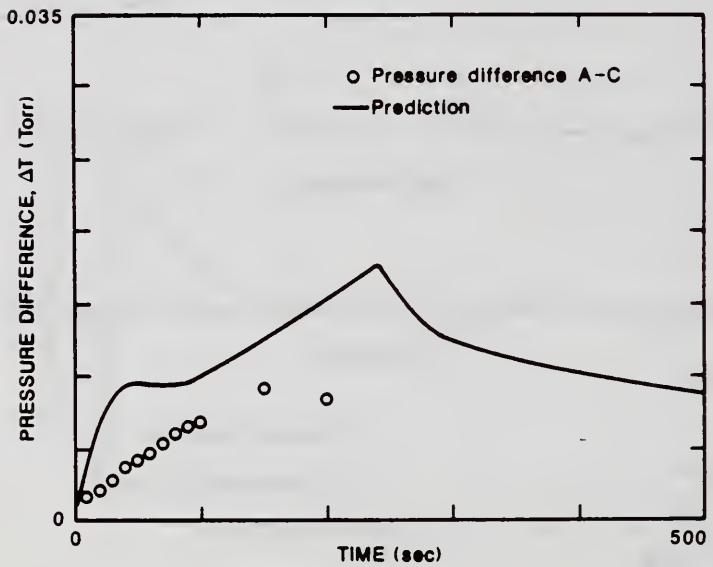

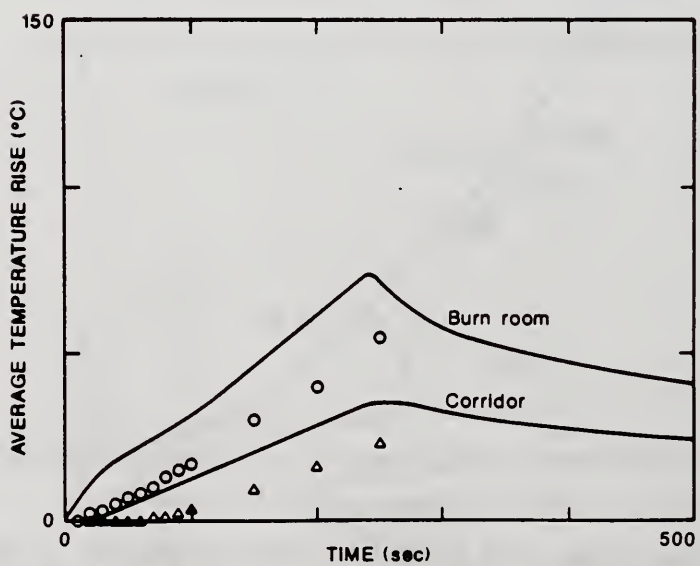

Figure 18b. Ramp fire, 1/2 Corridor configuration: λ, pressure difference and average temperature rises.

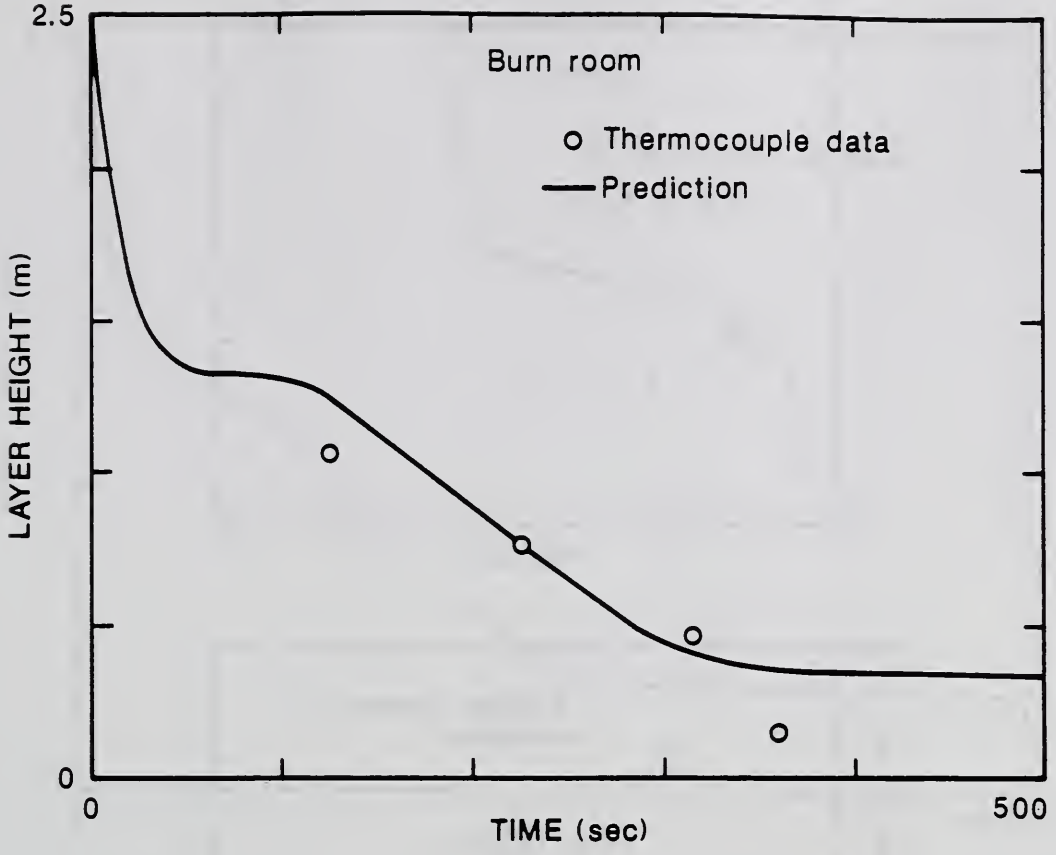

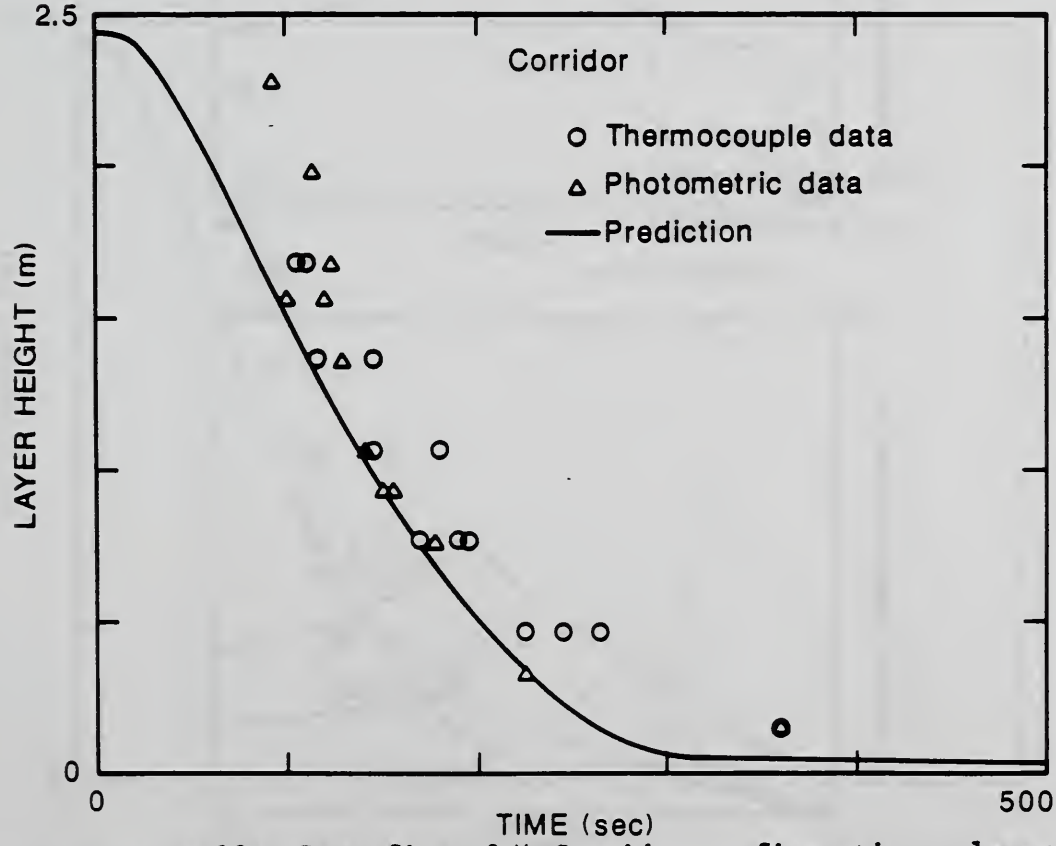

Figure 19a. Ramp fire, 3/4 Corridor configuration: layer heights.

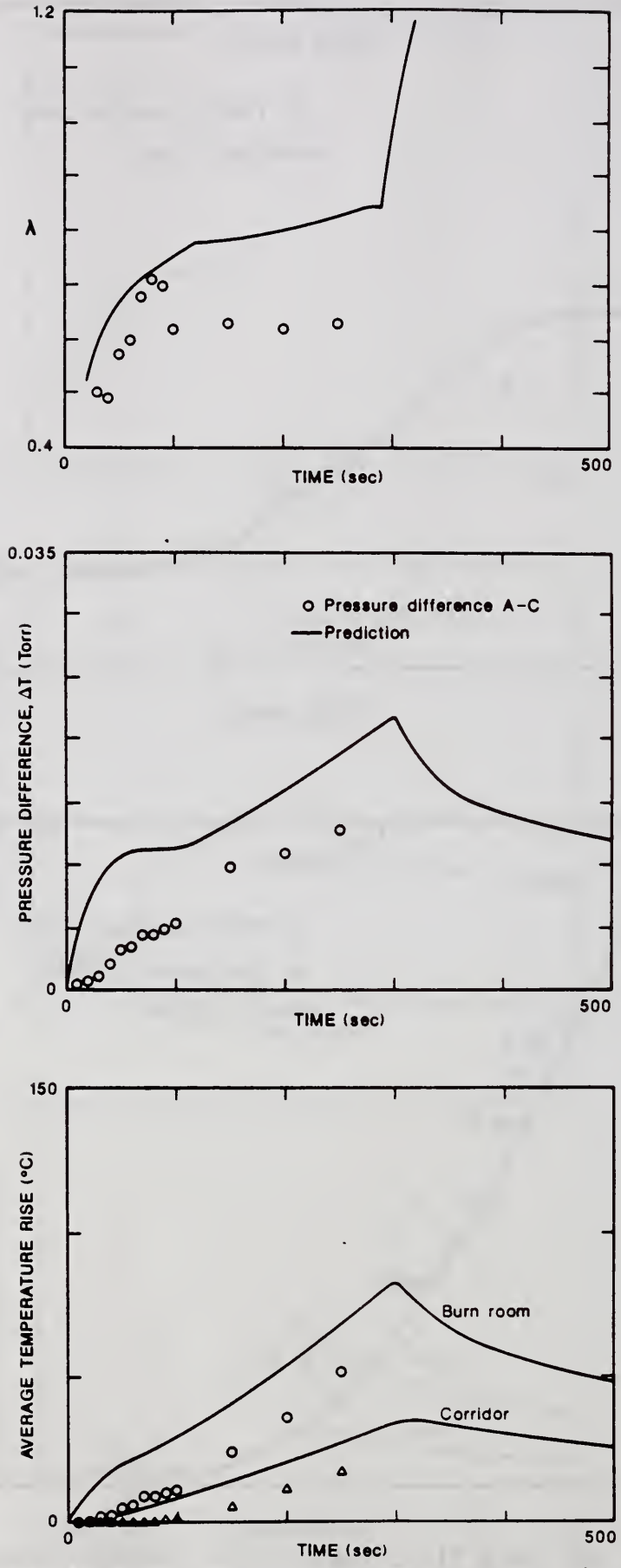

Figure 19b. Ramp fire, 3/4 Corridor configuration: λ, pressure difference and average temperature rises.

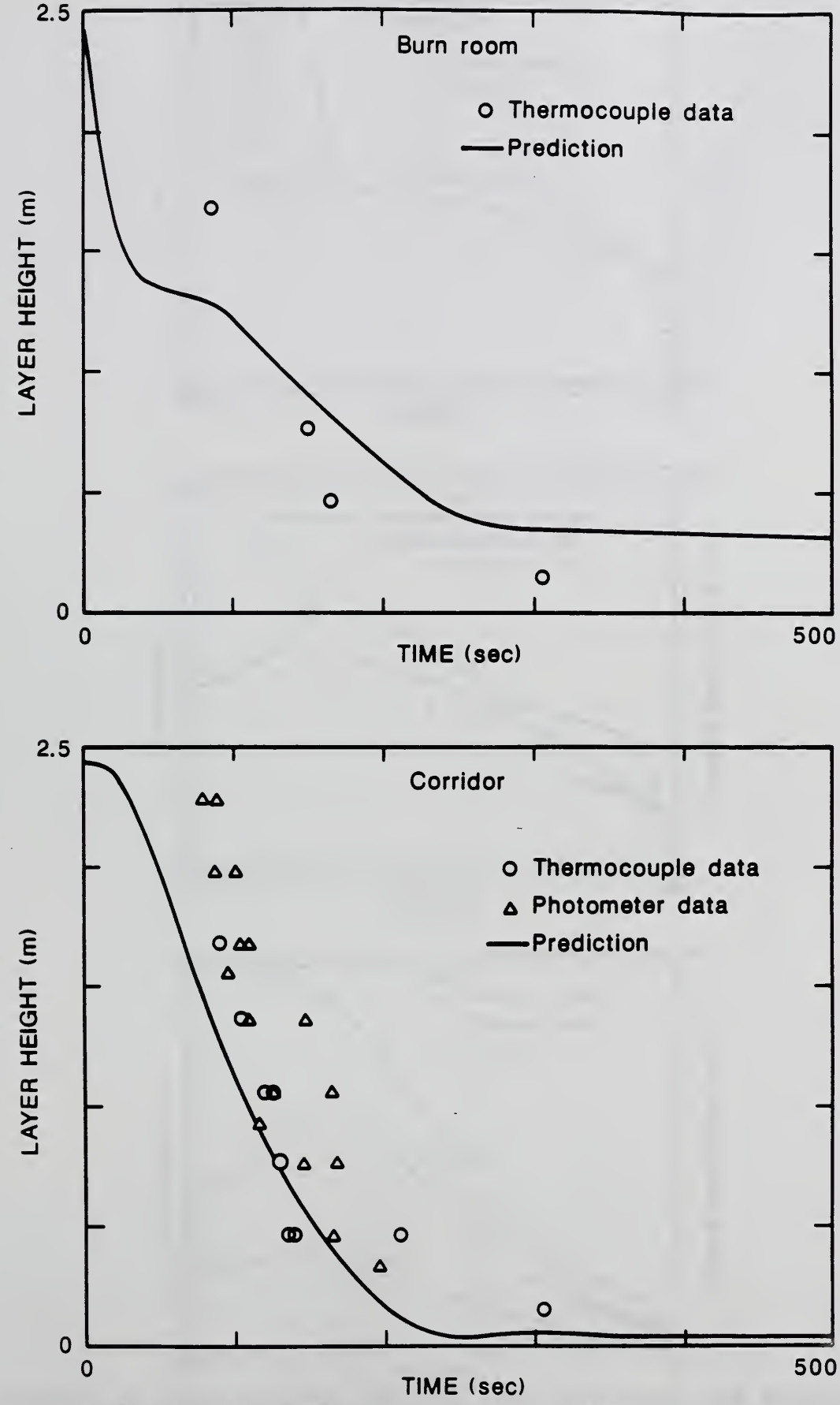

Figure 20a. Ramp fire, Full Corridor configuration: layer heights.

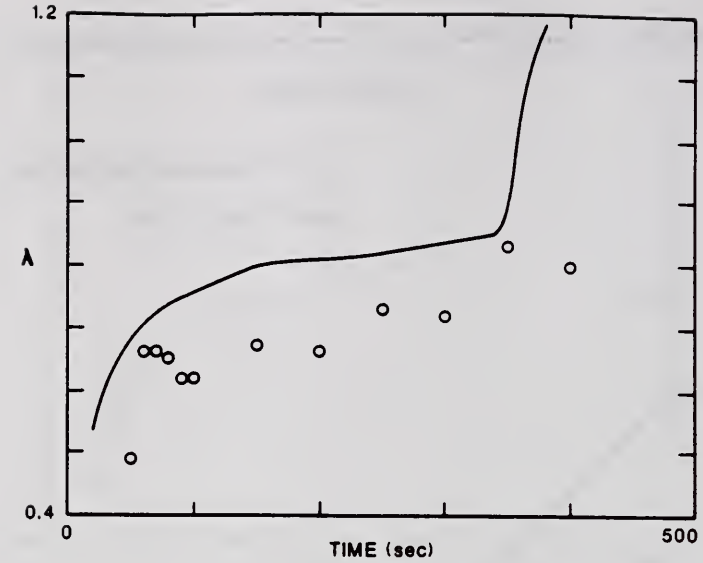

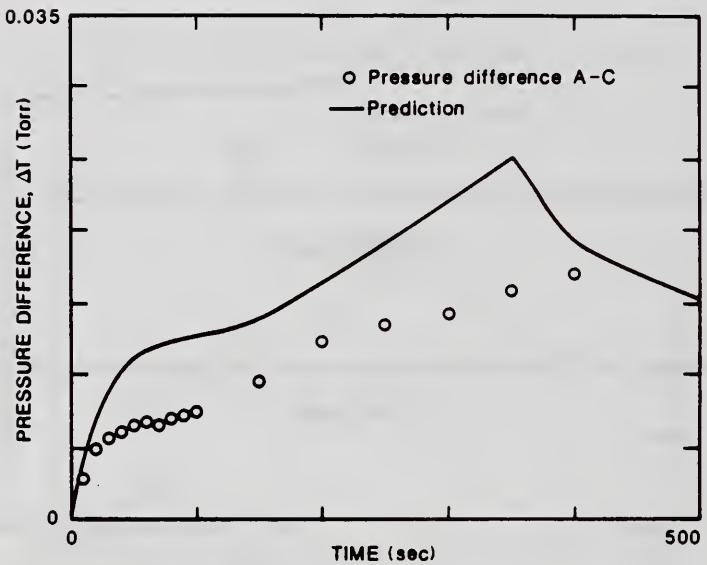

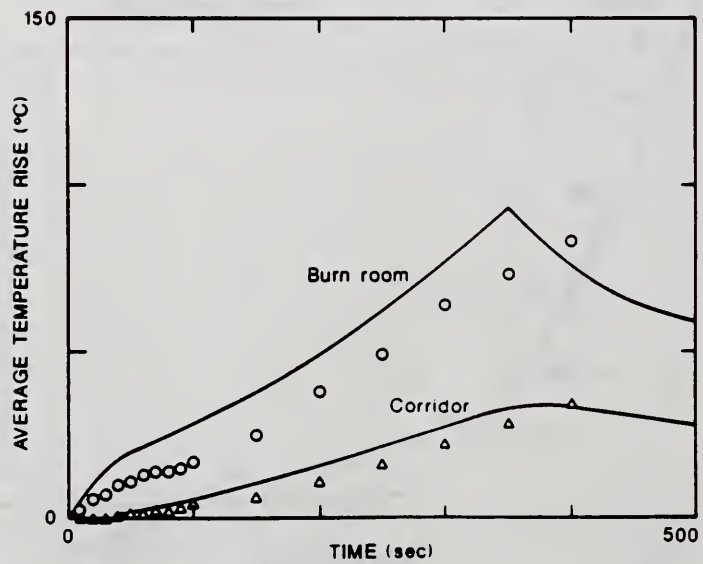

Figure 20b. Ramp fire, Full Corridor configuration: λ, pressure difference and average temperature rises.

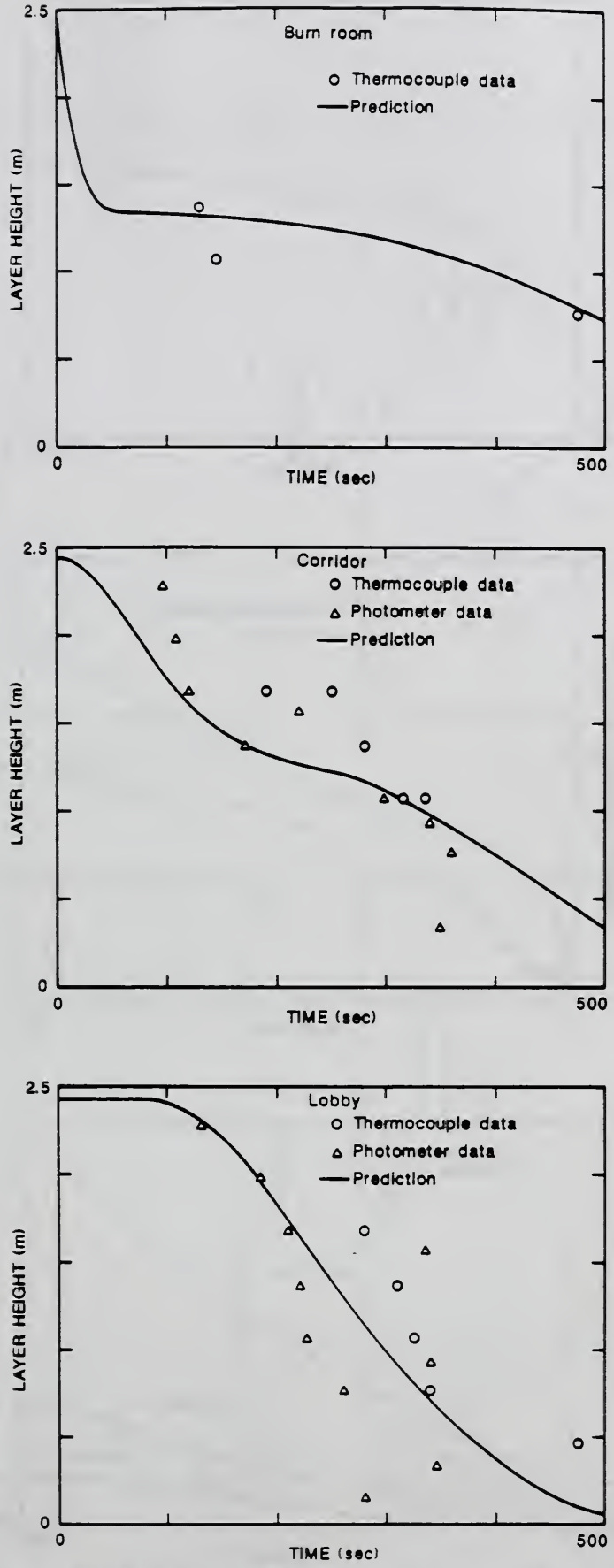

Figure 21a. Ramp fire, Corridor and Lobby configuration: layer heights.

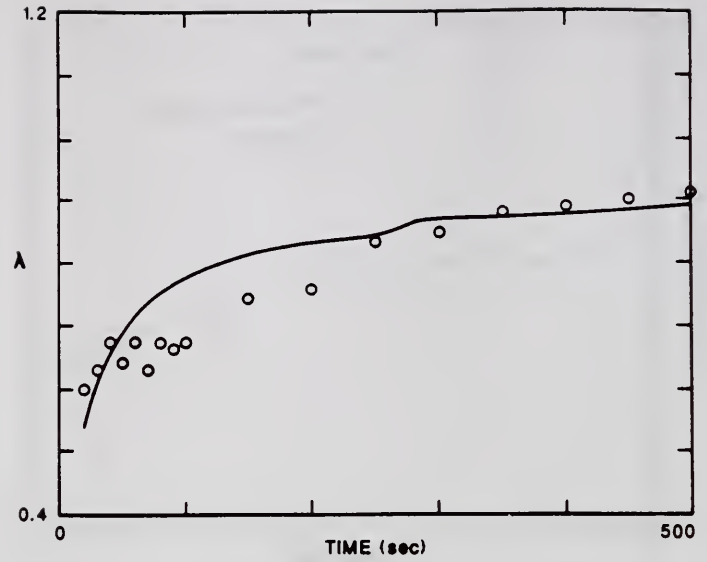

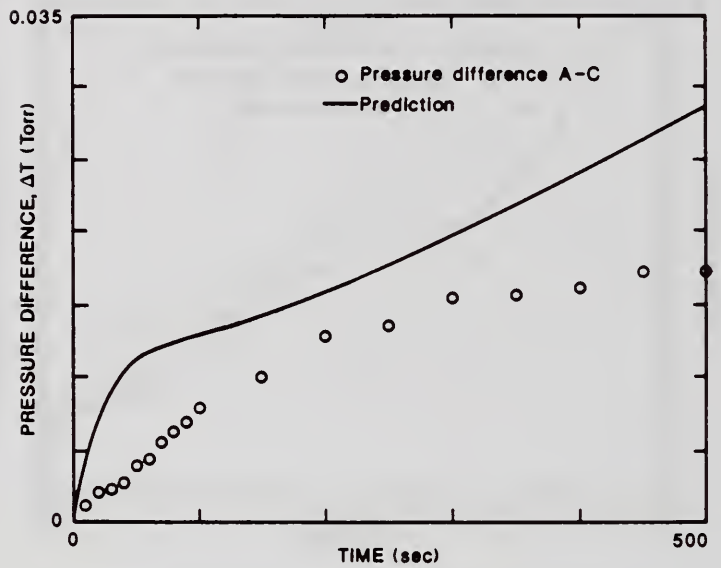

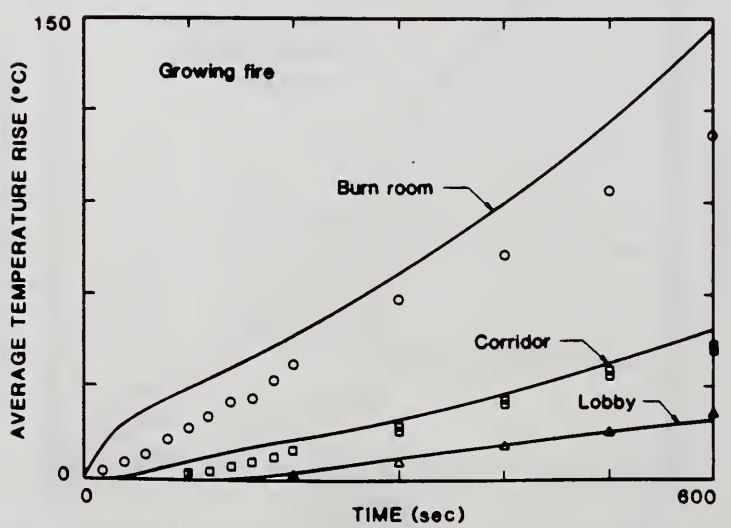

Figure 21b. Ramp fire, Corridor and Lobby configuration: λ, pressure difference and average temperature rises.

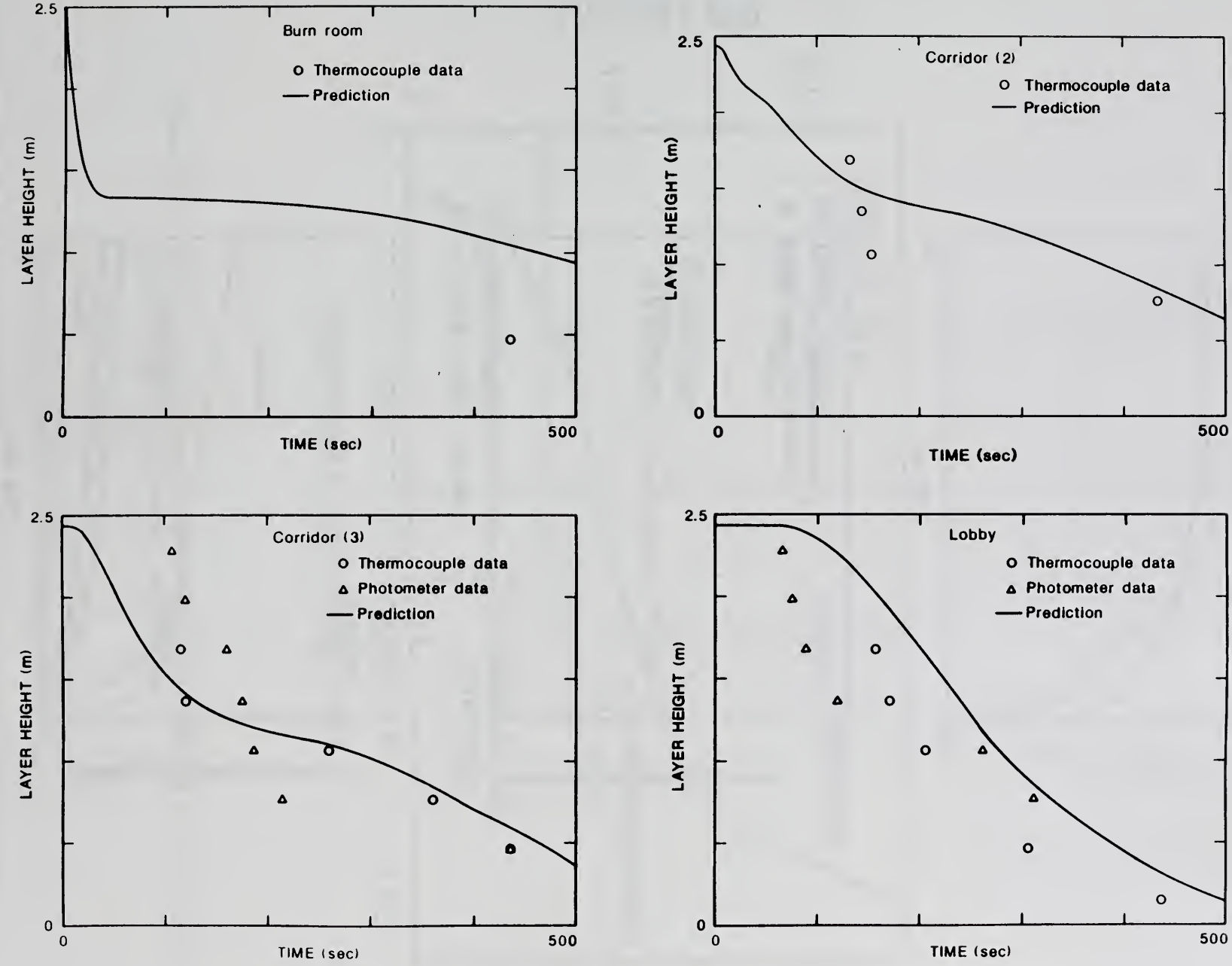

Figure 22a. 100 kW fire, Corridor (subdivided into 3 rooms) and Lobby: layer heights,

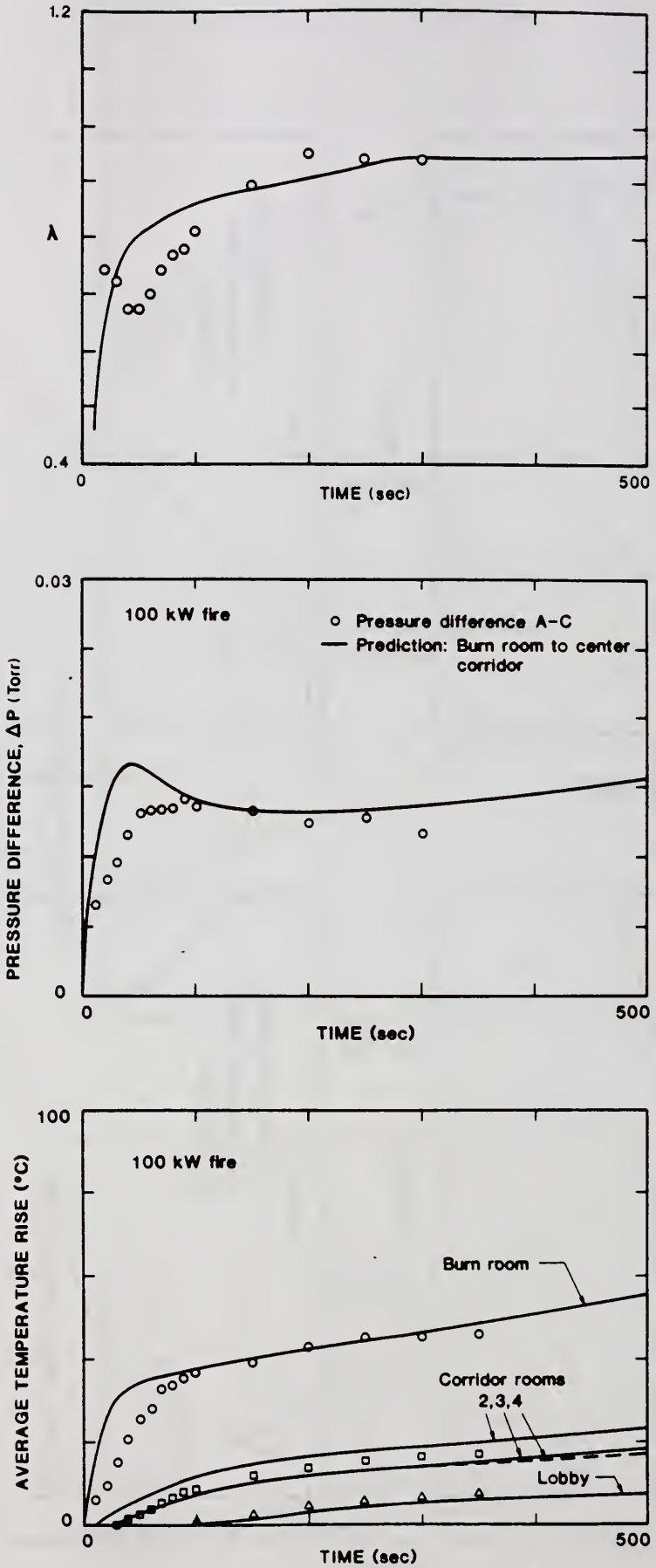

Figure 22b. 100 kW fire, Corridor (subdivided into 3 rooms) and Lobby: λ, pressure difference and average temperature rises.

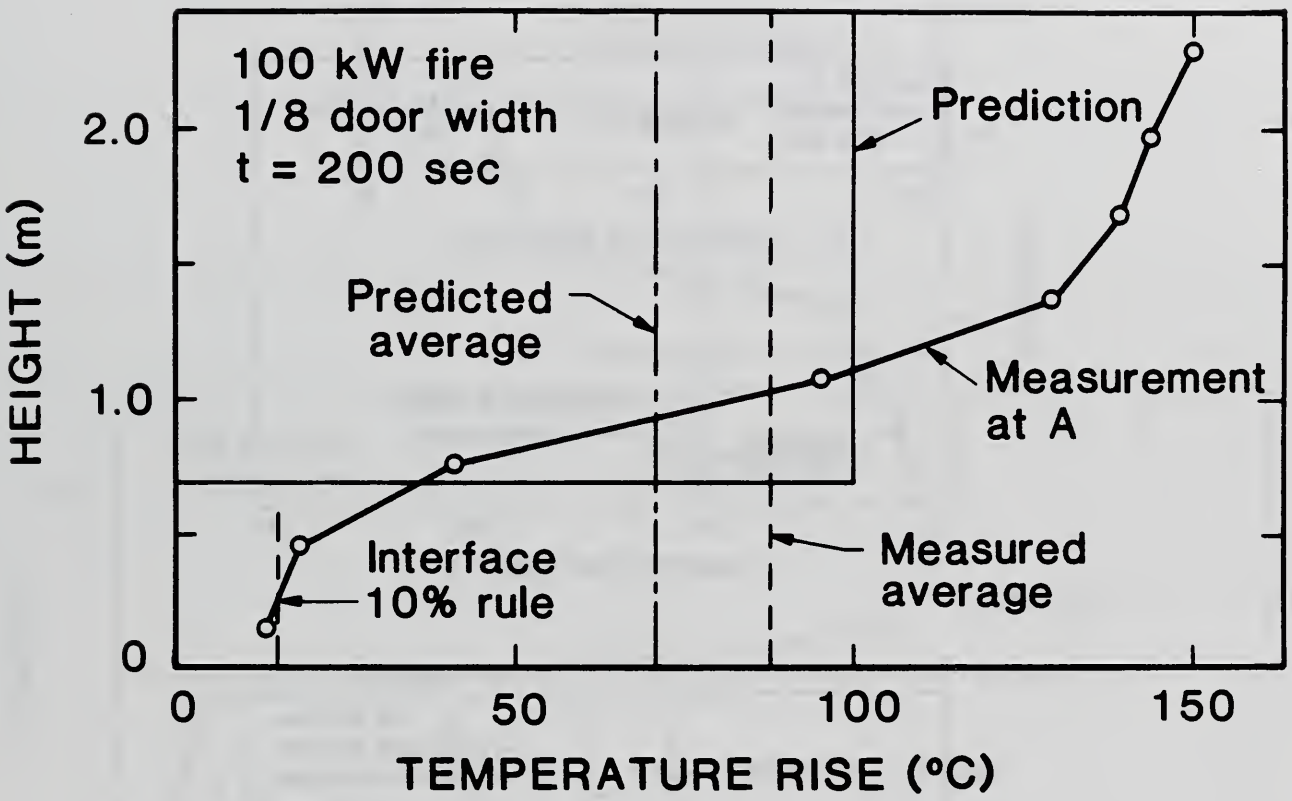

Figure 23. Burn room vertical temperature distribution at 200 seconds, 100 kW fire: 1/8 normal width door.

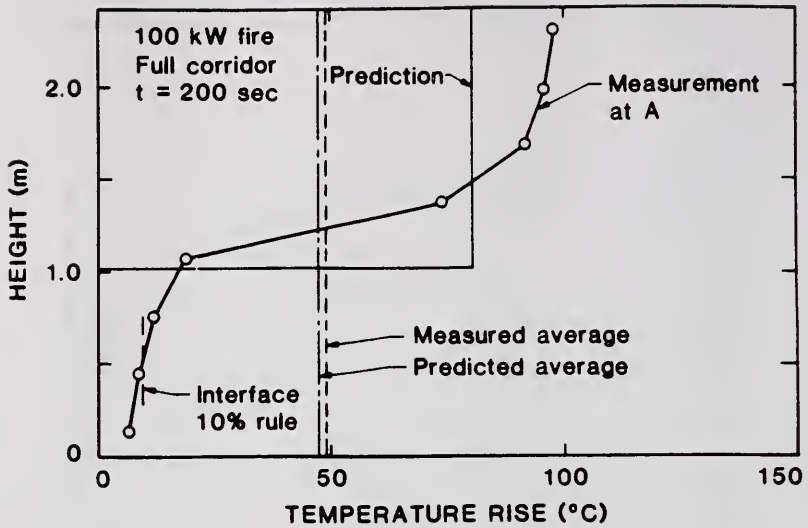

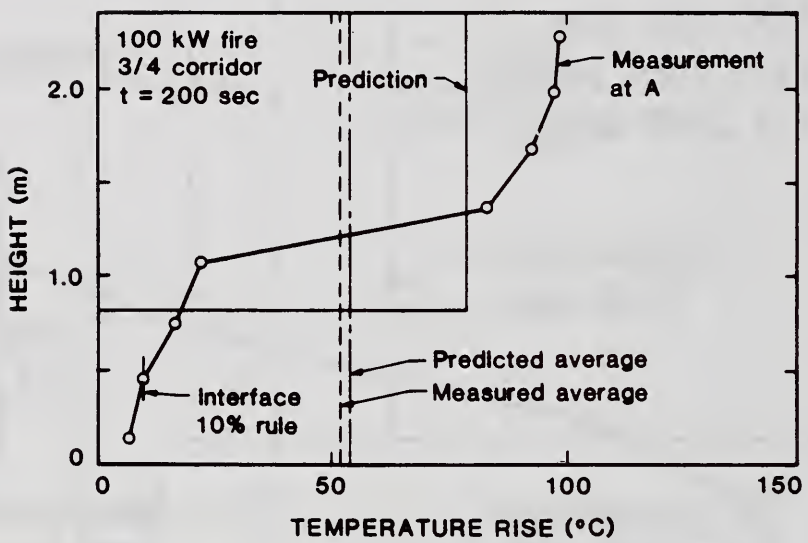

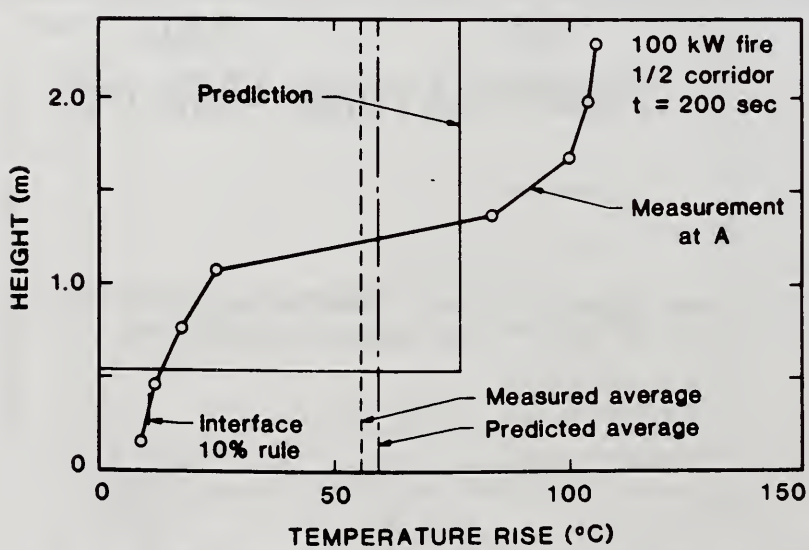

Figure 24. Burn room vertical temperature distribution at 200 seconds, normal door, 100 kW fire: full, 3/4 and 1/2 corridors sizes.

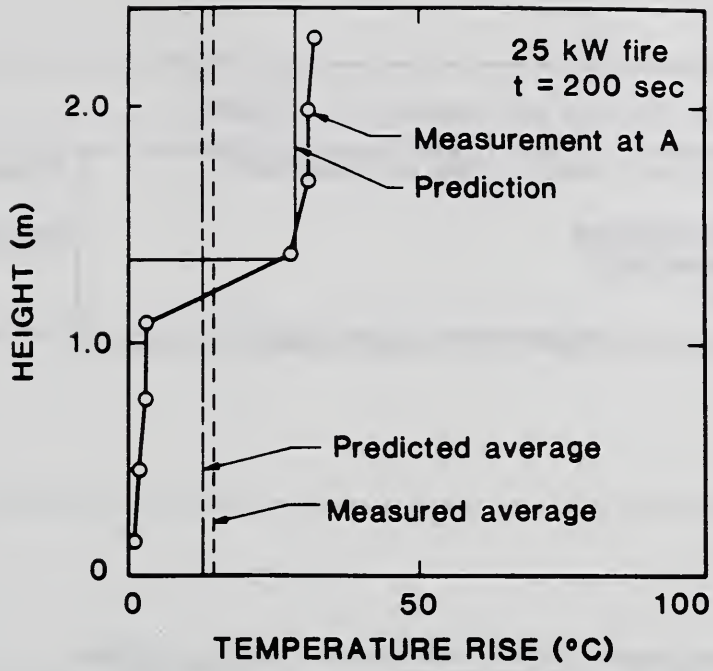

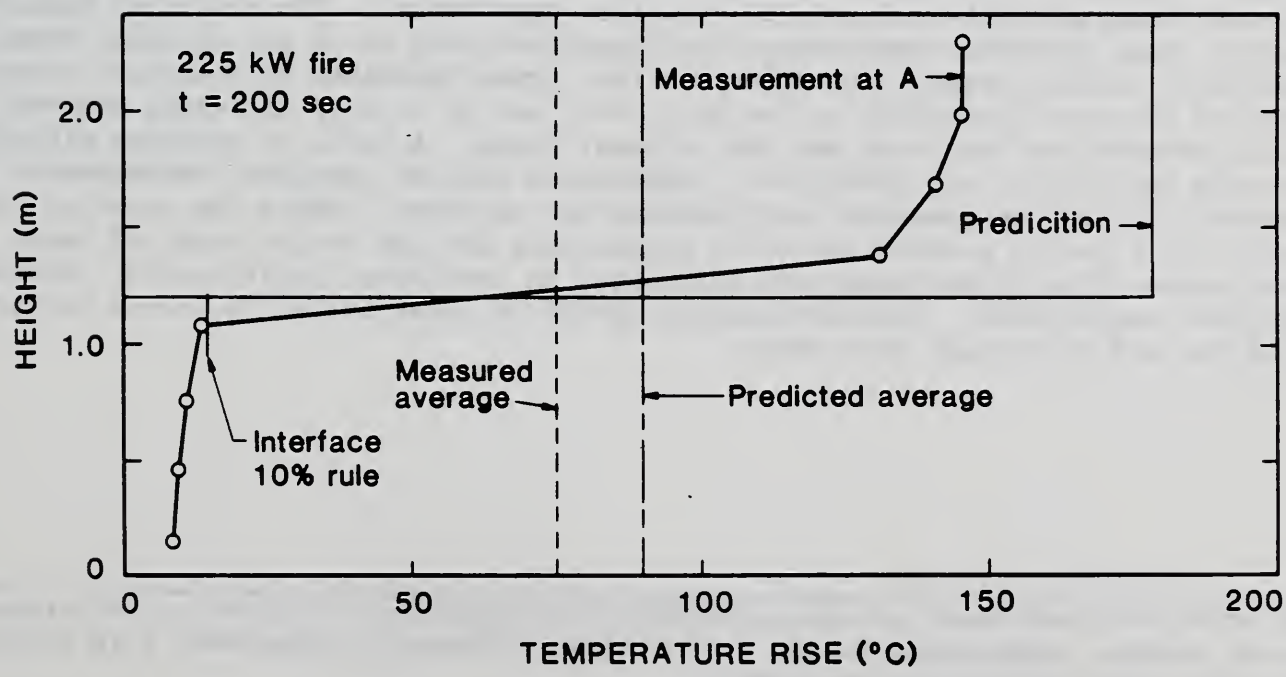

Figure 25. Burn room vertical temperature distribution at 200 seconds, normal door, corridor plus lobby: 25 and 225 kW fires.

NBS-114A (REV. 2-8C)

U.S. DEPT. OF COMM. BIBLIOGRAPHIC DATA SHEET (See instructions)	1. PUBLICATION OR REPORT NO. NBSIR-87-3567	2. Performing Organ. Report No.	3. Publication Date July 1987

4. TITLE AND SUBTITLE

Comparisons of NBS/Harvard VI Simulations and Full-Scale, Multi-Room Fire Test Data

5. AUTHOR(S)
John A. Rockett, Masahiro Morita and Leonard Y. Cooper

6. PERFORMING ORGANIZATION (If joint or other than NBS, see instructions)

NATIONAL BUREAU OF STANDARDS
U.S. DEPARTMENT OF COMMERCE
GAITHERSBURG, MD 20899

7. Contract/Grant No.

8. Type of Report & Period Covered

9. SPONSORING ORGANIZATION NAME AND COMPLETE ADDRESS (Street, City, State, ZIP)

10. SUPPLEMENTARY NOTES

☐ Document describes a computer program; SF-185, FIPS Software Summary, is attached.

11. ABSTRACT (A 200-word or less factual summary of most significant information. If document includes a significant bibliography or literature survey, mention it here)

The NBS/Harvard VI multiroom fire model computer code was used to simulate results of previously reported full-scale, multi-room fire experiments. The tests and simulations involved: four different compartment configurations made up of two or three rooms connected by open doorways, four different fire types generated by a methane burner located in the room identified as the burn room, and up to four different doorway openings between the burn room and the adjacent space. A total of nineteen different tests were carried out and simulated. Comparisons between simulated and measured parameters of the fire-generated environments are reviewed. While the computer code is generally found to provide excellent simulations for the entire range of tests, several areas in modeling detail are identified as requiring clarification, research, and further improvement. The improvements should be incorporated in future versions of the NBS/Harvard Multi-Room Fire Model.

12. KEY WORDS (Six to twelve entries; alphabetical order; capitalize only proper names; and separate key words by semicolons)
computer models; compartment fires; fire models; full-scale compartment fire experiments multi-room fires; simulation; validation

13. AVAILABILITY

☒ Unlimited

☐ For Official Distribution. Do Not Release to NTIS

☐ Order From Superintendent of Documents, U.S. Government Printing Office, Washington, D.C. 20402.

☒ Order From National Technical Information Service (NTIS), Springfield, VA. 22161

14. NO. OF PRINTED PAGES
66

15. Price
$13.95

USCOMM-DC 6043-P80